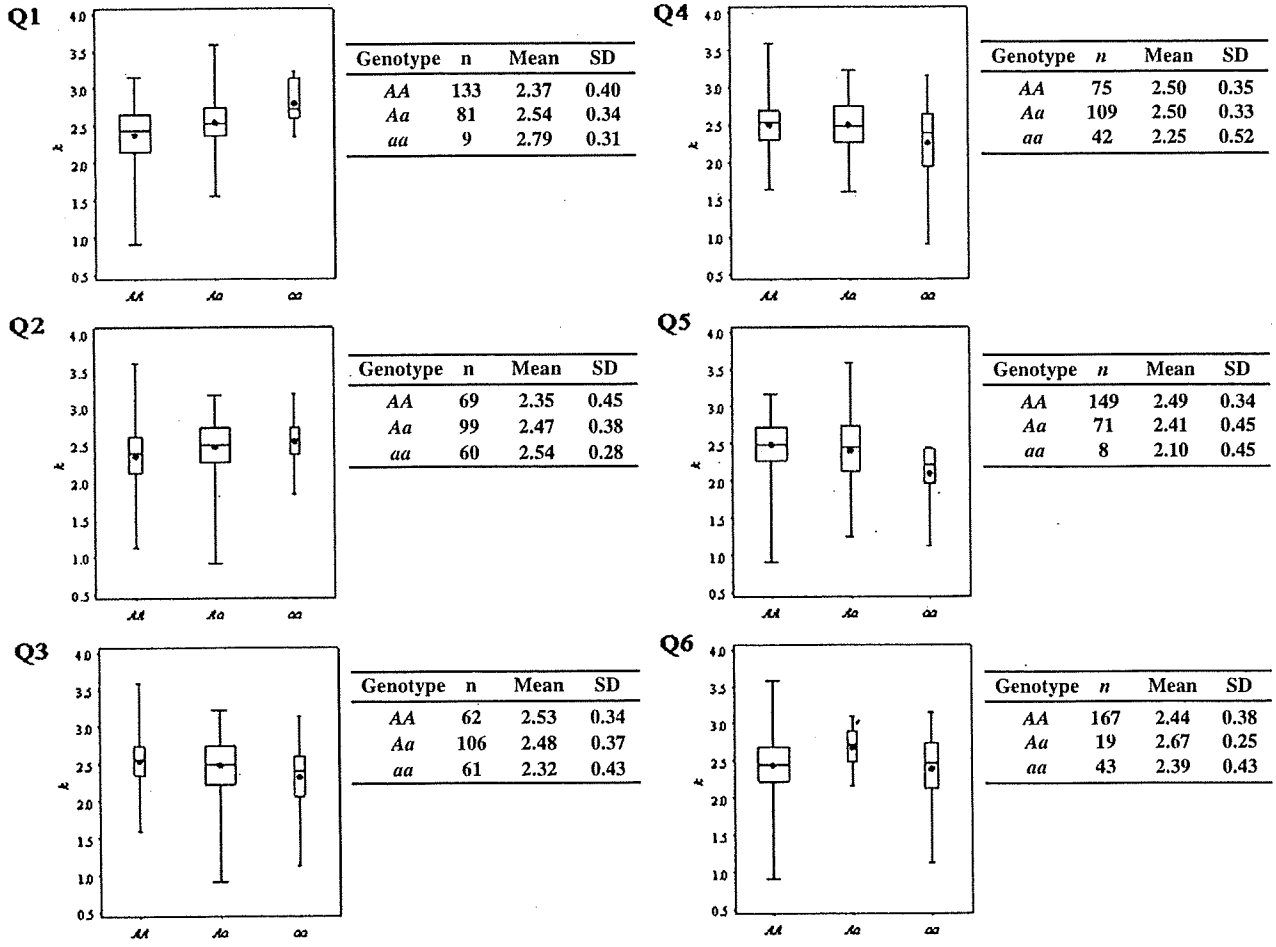

Figure 3 Summary statistics and box–whisker plot in questionnaire survey.

chosen as project targets: irinotecan, fluorouracil, paclitaxel and gemcitabine. One or some combination of the drugs was administered to about 1000 cancer patients with written informed consent at the National Cancer Center, Japan. PK data were also obtained for the drugs except for fluorouracil. In addition, about 1000 DNA samples were extracted from peripheral blood mononuclear cells and 109 365 SNPs were genotyped by Illumina Human-1 BeadChip.

In this application, we emphasize a focus on the gemcitabine pharmacogenomics study. Gemcitabine (2′,2′-difluorodeoxycytidine) is a nucleoside anticancer drug that has a broad spectrum of antitumor activity against various solid tumors, such as nonsmall cell lung cancer and pancreatic cancer. The participants consisted of 256 Japanese gemcitabine-naive cancer patients (mainly pancreatic carcinoma) at the National Cancer Center Hospital and National Cancer Center Hospital East. Details of this analysis group were reported previously.[27] For gemcitabine PK analysis, 5 ml of heparinized blood was sampled before the first gemcitabine administration, and at 0, 15, 30, 60, 90, 120 and 240 min after the termination of the infusion. The AUC, mean residence time from 0 to infinity, peak concentration (C_{max}), clearance (CL m^{-2}), distribution volume based on the terminal phase (Vz m^{-2}) and elimination rate constant (K_{el}) were calculated using WinNonlin ver. 4.01 (Pharsight Corporation, Mountain View, CA, USA). For an investigation of the association between these PK parameters and SNPs in Illumina Human-1 BeadChip, we applied the maximum contrast method, the modified maximum contrast method and the Kruskal–Wallis test.

Acknowledgments

We thank Professor Isao Yoshimura and Professor Chikuma Hamada at Tokyo University of Science for their valuable advice, and Dr Hiromi Sakamoto and Ms Sumiko Ohnami for the SNP genotyping. Yasunori Sato is a recipient of Official Trainee of the Foreign Clinical Pharmacology Training Program, Japanese Society of Clinical Pharmacology and Therapeutics. This work was initiated while Yasunori Sato was a postdoctoral fellow at the Department of Biostatistics, Harvard School of Public Health, and partially supported in Japan by the program for promotion of Fundamental Studies in Health Sciences of the National Institute of Biomedical Innovation (NiBio).

Duality of Interest

None declared.

References

1 Licinio J, Wong M. *Pharmacogenomics: The Search for Individualized Therapies*. Wiley: Weinheim (Germany), 2002.
2 Evans WE, McLeod HL. Pharmacogenomics—drug disposition, drug targets, and side effects. *N Engl J Med* 2003; **348**: 538–549.
3 Ingelman-Sundberg M. Pharmacogenomic biomarkers for prediction of severe adverse drug reactions. *N Engl J Med* 2008; **358**: 637–639.
4 Efferth T, Volm M. Pharmacogenetics for individualized cancer chemotherapy. *Pharmacol Ther* 2005; **107**: 155–176.
5 US FDA. Guidance for Industry Pharmacogenomic Data Submissions. 2005.
6 International Human Genome Sequencing Consortium. Finishing the euchromatic sequence of the human genome. *Nature* 2004; **431**: 931–945.
7 Risch N, Merikangas K. The future of genetic studies of complex human diseases. *Science* 1996; **273**: 1516–1517.
8 Hirschhorn JN, Daly MJ. Genome-wide association studies for common diseases and complex traits. *Nat Rev Genet* 2005; **6**: 95–108.
9 Kingsmore SF, Lindquist IE, Mudge J, Gessler DD, Beavis WD. Genome-wide association studies: progress and potential for drug discovery and development. *Nat Rev Drug Discov* 2008; **7**: 221–230.
10 Kruskal HW, Wallis WA. Use of ranks in one-criterion variance analysis. *J Am Stat Assoc* 1952; **47**: 583–621.
11 Siegel S, Castellan NJ. *Nonparametric Statistics for the Behavioral Sciences*, 2nd edn. McGraw-Hill: New York, 1988.
12 Mukerjee H, Robertson T, Wright FT. Comparison of several treatments with a control using multiple contrast. *J Am Stat Assoc* 1987; **82**: 902–910.
13 Ruberg SJ. Contrasts identifying the minimum effective dose. *J Am Stat Assoc* 1989; **82**: 816–822.
14 Yoshimura I, Wakana A, Hamada C. A performance comparison of maximum contrast methods to detect dose dependency. *Drug Inf J* 1997; **31**: 423–432.
15 Stewart H, Ruberg SJ. Detecting dose response with contrasts. *Stat Med* 2000; **19**: 913–921.
16 Nishiyama H, Yanagihara H, Yoshimura I. SAS/IML program for computing probabilities related to maximum contrast methods. *Jpn J Biometrics* 2003; **24**: 57–70, (in Japanese).
17 Wakana A, Yoshimura I, Hamada C. A method for therapeutic dose selection in a phase II clinical trial using contrast statistics. *Stat Med* 2007; **26**: 498–511.
18 Jeunemaitre X, Soubrier F, Kotelevtsev YV, Lifton RP, Williams CS, Charru A *et al.* Molecular basis of human hypertension: role of angiotensinogen. *Cell* 1992; **71**: 169–180.
19 Caulfield M, Lavender P, Farrall M, Munroe P, Lawson M, Turner P *et al.* Linkage of the angiotensinogen gene to essential hypertension. *N Engl J Med* 1994; **330**: 1629–1633.
20 Hegele RA, Brunt JH, Connelly PW. A polymorphism of the angiotensinogen gene associated with variation in blood pressure in a genetic isolate. *Circulation* 1994; **90**: 2207–2212.
21 Vasku A, Soucek M, Znojil V, Rihacek I, Tschoplova S, Strelcova L *et al.* Angiotensin I-converting enzyme and angiotensinogen gene interaction and prediction of essential hypertension. *Kidney Int* 1998; **53**: 1479–1482.
22 Pereira TV, Nunes AC, Rudnicki M, Yamada Y, Pereira AC, Krieger JE. Meta-analysis of the association of 4 angiotensinogen polymorphisms with essential hypertension: a role beyond M235T? *Hypertension* 2008; **51**: 778–783.
23 Pei Y, Scholey J, Thai K, Suzuki M, Cattran D. Association of angiotensinogen gene T235 variant with progression of immunoglobulin A nephropathy in Caucasian patients. *J Clin Invest* 1997; **100**: 814–820.
24 Genz A, Bretz F. Numerical computation of multivariate t-probabilities with application to power calculation of multiple contrasts. *J Stat Comput Simulat* 1999; **63**: 361–378.
25 Westfall PH, Young SS. *Resampling-Based Multiple Testing: Examples and Methods for P-value Adjustment*. Wiley: New York, 1993.
26 Gabrielsson J, Weiner D. *Pharmacokinetic and Pharmacodynamic Data Analysis: Concepts and Applications*. Taylor & Francis: Sweden, 2000.
27 Sugiyama E, Kaniwa N, Kim SR, Kikura-Hanajiri R, Hasegawa R, Maekawa K *et al.* Pharmacokinetics of gemcitabine in Japanese cancer patients: the impact of a cytidine deaminase polymorphism. *J Clin Oncol* 2007; **25**: 32–42.

VOLUME 27 · NUMBER 13 · MAY 1 2009

JOURNAL OF CLINICAL ONCOLOGY

ORIGINAL REPORT

Identification of a Predictive Biomarker for Hematologic Toxicities of Gemcitabine

Junichi Matsubara, Masaya Ono, Ayako Negishi, Hideki Ueno, Takuji Okusaka, Junji Furuse, Koh Furuta, Emiko Sugiyama, Yoshiro Saito, Nahoko Kaniwa, Junichi Sawada, Kazufumi Honda, Tomohiro Sakuma, Tsutomu Chiba, Nagahiro Saijo, Setsuo Hirohashi, and Tesshi Yamada

From the Chemotherapy Division, National Cancer Center Research Institute; Hepatobiliary and Pancreatic Oncology Division and Clinical Laboratory Division, National Cancer Center Hospital; Project Team for Pharmacogenetics, National Institute of Health Sciences; BioBusiness Group, Mitsui Knowledge Industry, Tokyo; Hepatobiliary and Pancreatic Oncology Division, National Cancer Center Hospital East, Kashiwa; and Department of Gastroenterology and Hepatology, Kyoto University Graduate School of Medicine, Kyoto, Japan.

Submitted September 3, 2008; accepted December 1, 2008; published online ahead of print at www.jco.org on March 16, 2009.

Supported by the Program for Promotion of Fundamental Studies in Health Sciences conducted by the National Institute of Biomedical Innovation of Japan, the Third-Term Comprehensive Control Research for Cancer conducted by the Ministry of Health and Labor of Japan, and generous grants from the Naito Foundation, the Princess Takamatsu Cancer Research Fund, and the Foundation for the Promotion of Cancer Research. These sponsors had no role in the design of the study, the collection of the data, the analysis and interpretation of the data, the decision to submit the article for publication, or the writing of the article

Authors' disclosures of potential conflicts of interest and author contributions are found at the end of this article.

Corresponding author: Tesshi Yamada, MD, PhD, Chemotherapy Division, National Cancer Center Research Institute, 5-1-1 Tsukiji, Chuo-ku, Tokyo 104-0045, Japan; e-mail: tyamada@ncc.go.jp.

The Appendix is included in the full-text version of this article, available online at www.jco.org. It is not included in the PDF version (via Adobe® Reader®).

0732-183X/09/2713-2261/$20.00

DOI: 10.1200/JCO.2008.19.9745

ABSTRACT

Purpose
Gemcitabine monotherapy is the current standard for patients with advanced pancreatic cancer, but the occurrence of severe neutropenia and thrombocytopenia can sometimes be life threatening. This study aimed to discover a new diagnostic method for predicting the hematologic toxicities of gemcitabine.

Patients and Methods
Using quantitative mass spectrometry (MS), we compared the baseline plasma proteomes of 25 patients who had developed severe hematologic adverse events (grade 3 to 4 neutropenia and/or grade 2 to 4 thrombocytopenia) within the first two cycles of gemcitabine with those of 22 patients who had not (grade 0).

Results
We identified 757 peptide peaks whose intensities were significantly different ($P < .001$, Welch t test) among a total of 60,888. The MS peak with the highest statistical significance ($P = .0000282$) was revealed to be derived from haptoglobin by tandem MS. A scoring system (nomogram) based on the values of haptoglobin, haptoglobin phenotype, neutrophil count, platelet count, and body-surface area was constructed to estimate the risk of hematologic adverse events (grade 3 to 4 neutropenia and/or grade 2 to 4 thrombocytopenia) with an area under curve value of 0.782 in a cohort of 166 patients with pancreatic cancer. Predictive ability of the system was confirmed in two independent validation cohorts consisting of 87 and 52 patients with area under the curve values of 0.655 and 0.747, respectively.

Conclusion
Although the precise mechanism responsible for the correlation of haptoglobin with the future onset of hematologic toxicities remains to be clarified, our prediction model seems to have high practical utility for tailoring the treatment of patients receiving gemcitabine.

J Clin Oncol 27:2261-2268. © 2009 by American Society of Clinical Oncology

INTRODUCTION

Pancreatic adenocarcinoma is one of the most aggressive and lethal cancers.[1] It is the fifth leading cause of cancer-related mortality in Japan and the fourth leading cause in the United States, accounting for an estimated more than 23,000 annual deaths in Japan and more than 33,000 deaths in the United States.[2,3] The median survival time of patients with advanced pancreatic cancer had remained at only 3 to 4 months until the introduction of the nucleoside anticancer drug gemcitabine (2′,2′-difluorodeoxycytidine). Gemcitabine monotherapy extended the overall survival of pancreatic cancer patients up to 6 months, along with significant clinical benefits such as pain relief and improvement of performance status,[4-6] and is now accepted as a standard first-line treatment for unresectable advanced pancreatic cancer.[7] However, hematologic toxicity is the dose-limiting factor of gemcitabine therapy.[8] Although severe nonhematologic toxicity is infrequent,[4-6] 20% to 30% of patients receiving gemcitabine experience grade 3 to 4 neutropenia (National Cancer Institute [NCI] Common Toxicity Criteria, version 2.0), and approximately 10% experience grade 3 to 4 thrombocytopenia.[5,6,9,10] These levels of severe hematologic adverse events (AEs) can be potentially life threatening.

Several attempts have been made to predict the occurrence of AE associated with chemotherapy. Old age, poor performance status, and reduced initial blood cell counts have been reported to be the risk factors of hematotoxicities.[11,12] To further improve prediction accuracy, combinations of these

risk factors have also been proposed,[11-14] but no reliable predictor has been established for gemcitabine-induced hematologic AEs. We previously identified a significant correlation of a nonsynonymous single nucleotide polymorphism of the cytidine deaminase (*CDA*) gene with altered pharmacokinetics of gemcitabine, but its prediction accuracy for hematologic AE was not satisfactory.[15,16]

Recent advanced proteomic technologies have been increasingly applied to studies of clinical samples[17] to identify biomarkers that could facilitate the tailoring of cancer treatments. Protein expression is not always correlated with mRNA expression,[18] and it is anticipated that alterations in the protein content of clinical samples more directly reflect the biologic and pathologic status of patients. Matrix-assisted laser desorption/ionization mass spectrometry (MS) is becoming a method of choice for profiling of clinical samples as a result of its high sensitivity and throughput. In fact, previous studies have successfully identified biomarkers that could predict the outcome of cancer patients and the efficacy of molecular-targeting drugs.[19,20] However, only low molecular weight proteins can be analyzed by matrix-assisted laser desorption/ionization MS, and thus, a method allowing more comprehensive protein profiling is desirable.

Shotgun proteomics is an emerging concept in which whole proteins are enzymatically digested into a large array of small peptide fragments having uniform physical and chemical characteristics and then analyzed directly by MS. We previously developed a new platform, namely two-dimensional image converted analysis of liquid chromatography and mass spectrometry (2DICAL), to give a quantitative dimension to shotgun proteomics.[21] To identify new biomarkers that might be useful for prediction of gemcitabine-induced neutropenia and thrombocytopenia in patients with pancreatic cancer, we compared the plasma protein profiles of two extreme populations of patients who had shown different responses to the same gemcitabine treatment by 2DICAL. Here we report the identification of plasma/serum haptoglobin as a biomarker of hematologic toxicities associated with gemcitabine treatment.

PATIENTS AND METHODS

Patients

Plasma or serum samples were collected from three cohorts (modeling [M0], validation-1 [V1], and validation-2 [V2] cohorts) totaling 305 patients. All the patients had locally advanced or metastatic (stage IVA or IVB),[22] histologically or cytologically proven pancreatic ductal adenocarcinoma and received at least two cycles of gemcitabine monotherapy (1,000 mg/m^2 intravenously over 30 minutes on days 1, 8, and 15 of a 28-day cycle). Demographic and laboratory data for the patients before administration of gemcitabine are listed in Appendix Tables A1 to A3 (online only). The severity of early hematologic AEs that appeared within the first two cycles of the gemcitabine treatment was graded according to NCI Common Terminology Criteria for Adverse Events (CTCAE; version 3.0).

Cohort M0 comprised 166 patients who had been enrolled onto our previous study at the National Cancer Center (NCC) Hospital (Tokyo, Japan) and Hospital East (Kashiwa, Japan) between September 2002 and July 2004.[15,16] Cohort V1 comprised 87 patients who had been treated consecutively at the NCC Hospital between August 2005 and June 2007, and cohort V2 comprised 52 patients treated at the NCC Hospital consecutively between August 2004 and July 2005.

Sample Preparation

Blood was drawn before the administration of gemcitabine. Plasma (cohorts M0 and V1) or serum (cohort V2) was separated by centrifugation at 4°C and frozen at −70°C (cohort M0) or −20°C (cohorts V1 and V2) until analysis. Macroscopically hemolyzed samples were excluded from the current analysis. The protocol of this retrospective study was reviewed and approved by the institutional ethics committee boards of the NCC (Tokyo, Japan) and the National Institute of Health Sciences (Tokyo, Japan).

Liquid Chromatography/MS

Samples were passed through an IgY-12 High Capacity Spin Column (Beckman Coulter, Fullerton, CA) in accordance with the manufacturer's instructions to reduce the amounts of the 12 most abundant plasma proteins. The flow-through portion was digested with sequencing-grade modified trypsin (Promega, Madison, WI) and analyzed in triplicate using a nano-flow high-performance liquid chromatograph (NanoFrontier nLC; Hitachi High-Technologies, Tokyo, Japan) connected to an electrospray ionization quadrupole time-of-flight (ESI-Q-TOF) mass spectrometer (Q-Tof Ultima; Waters, Milford, MC).

MS peaks were detected, normalized, and quantified using the in-house 2DICAL software package, as described previously.[21] A serial identification (ID) number was applied to each of the MS peaks detected (1 to 60,888). The stability of liquid chromatography/MS was monitored by calculating the correlation coefficient of every triplicate measurement. The mean correlation coefficient (±standard deviation) of the entire 60,888 peaks of the 47 triplicate runs was as high as 0.978 (±0.017).

Tandem MS

Peak lists were generated using the Mass Navigator software package (version 1.2; Mitsui Knowledge Industry, Tokyo, Japan) and searched against the SwissProt database (downloaded from http://www.expasy.ch/sprot/sprot-top.html on October 18, 2007) using the Mascot software package (version 2.2.1; Matrix Science, London, United Kingdom). The score threshold was set to $P < .05$ based on the size of the database used in the search.

Western Blot Analysis

Primary antibodies used were rabbit polyclonal antibody against human haptoglobin (Dako, Glostrup, Denmark) and mouse monoclonal antibody against human complement C3b-α (Progen, Heidelberg, Germany). Ten microliters of partitioned sample were separated by sodium dodecyl sulfate–polyacrylamide gel electrophoresis (SDS-PAGE) and electroblotted onto a polyvinylidene difluoride membrane. The membrane was then incubated with the primary antibody and subsequently with relevant horseradish peroxidase–conjugated antirabbit or antimouse immunoglobulin G as described previously.[23,24] Blots were developed using an enhanced chemiluminescence (ECL) detection system (GE Healthcare, Buckinghamshire, United Kingdom).

Quantification and Subtyping of Haptoglobin

The concentration of plasma or serum haptoglobin was measured using an automated immunonephelometry BN-II system (Siemens Healthcare Diagnostics, Tokyo, Japan). The phenotype of haptoglobin α-chain was determined by nondenaturing (native) SDS-PAGE.[25]

Categorization of Hematologic Toxicities

Overall severity of hematologic toxicities after gemcitabine treatment was classified into categories I to IV based on the worst CTCAE grades of neutropenia and thrombocytopenia (Appendix Fig A1, online only), as follows: category I, grade 0 to 1 neutropenia and grade 0 thrombocytopenia; category II, grade 2 neutropenia or grade 1 thrombocytopenia; category III, grade 3 neutropenia or grade 2 thrombocytopenia; and category IV, grade 4 neutropenia or grade 3 to 4 thrombocytopenia.

Statistical Analysis

Statistical significance of intergroup differences was assessed using the Welch t test, χ^2 test, Wilcoxon test, or Kruskal-Wallis test, as appropriate. Multivariate regression analysis was performed using ordinal logistic regression modeling. Factors included in the prediction model were selected with a forward stepwise selection procedure using Akaike's Information Criterion (AIC). To correct biased sample sizes of categories, each observation was weighted according to the sample size of its category in the fitting process. The significance of differences between models with and without haptoglobin was assessed with the likelihood ratio test. Statistical analyses were performed using

an open-source statistical language R (version 2.7.0; http://www.r-project.org/) with the optional module design package.

RESULTS

Plasma Proteins Associated With Hematologic AEs

To identify a biomarker that can predict the occurrence of hematologic AEs associated with gemcitabine treatment, we compared the baseline plasma proteome between 25 patients who developed severe AEs (grade 3 to 4 neutropenia and/or grade 2 to 4 thrombocytopenia) and 22 patients who did not (grade 0) using 2DICAL. These levels of hematologic AEs have been used as criteria for dose reduction or postponement of gemcitabine-based treatments.[26-28] There was no significant difference in age, sex, Eastern Cooperative Oncology Group performance status, routine biochemical laboratory data, or pharmacokinetics of gemcitabine[15] (Table 1 and data not shown) between the two extreme groups of patients who were selected from cohort M0, but the patients who experienced severe AEs had significantly lower baseline peripheral-blood leukocyte, neutrophil, and platelet counts than patients without AEs (Table 1).

Among a total of 60,888 independent MS peaks detected within the range of 250 to 1,600 m/z and within the time range 20 to 70 minutes, we found that the mean intensity of triplicates differed significantly in 757 peaks ($P < .001$, Welch t test). Figure 1A is a representative two-dimensional view of all the MS peaks displayed with m/z along the x-axis and the retention time of LC along the y-axis. The 757 MS peaks whose expression differed significantly between patients with severe AEs and patients without AEs are highlighted in red.

One hundred fifteen MS/MS spectra acquired from 200 peaks with the smallest P values were matched to 41 proteins in the database (Mascot score of > 15; Appendix Tables A4 and A5, online only). Notably, MS peaks including one that was decreased in patients with severe AEs with the highest statistical significance ($P = .0000282$; Fig 1B) most recurrently (six times) matched the amino acid sequences of the haptoglobin (*HP*) gene product (Appendix Fig A2, online only). Figure 2A shows the distribution of two representative haptoglobin-derived MS peaks (ID 2062 [at 491 m/z and 44.5 minutes] and ID 5681 [at 602 m/z and 47 minutes]) in patients with severe AEs and without AEs. The differential expression and identification of haptoglobin were confirmed by denaturing SDS-PAGE and immunoblotting (Fig 2B).

Correlation of Haptoglobin With the Degree of Hematologic Toxicities

The levels of haptoglobin in plasma or serum samples obtained from 305 patients with advanced pancreatic cancer before gemcitabine treatment were measured by immunonephelometry and compared with the occurrence and severity of hematologic AEs. Consistent with 2DICAL analysis, the plasma levels of haptoglobin were significantly lower in the 25 patients with severe AEs than in the 22 patients without AEs ($P = .0002$, Wilcoxon test; Table 1).

The plasma level of haptoglobin showed a significant correlation with the NCI-CTCAE grade of neutropenia ($P = .012$, Kruskal-Wallis test) and hematologic toxicity categories ($P = .001$) in the 166 patients of cohort M0 (Fig 3A and Appendix Table A1). The correlation of haptoglobin levels with the grades of neutropenia and thrombocytopenia as well as the toxicity categories was consistently observed in the

Table 1. Clinical and Laboratory Data of Patients Without AEs and With Severe AEs

Factor	Patients Without AEs (n = 22)	Patients With Severe AEs (n = 25)	P
Haptoglobin, mg/dL			.0002
Mean	286	155	
SD	130	59	
Haptoglobin phenotype, No. of patients			.705*
Hp 2-2	12	14	
Hp 2-1	8	7	
Hp 1-1	2	4	
Sex, No. of patients			.344*
Male	12	17	
Female	10	8	
Age, years			.616
Mean	64	63	
SD	8	8	
ECOG performance status, No. of patients			.862*
0	12	13	
1	10	12	
2	0	0	
Body-surface area, m^2			.733
Mean	1.51	1.53	
SD	0.20	0.18	
Prior therapy, No. of patients			.867*
None	19	22	
Chemoradiotherapy using FU for LAPC	3	3	
Leucocyte, $\times 10^3/\mu L$			0002
Mean	7.4	4.8	
SD	2.8	1.4	
Absolute neutrophil count, $\times 10^3/\mu L$			.0002
Mean	5.3	3.0	
SD	2.4	1.1	
Platelet, $\times 10^4/\mu L$			< .0001
Mean	28	17	
SD	11	6	
Hemoglobin, g/dL			.806
Mean	12.1	11.9	
SD	1.4	1.4	
Albumin, g/dL			.131
Mean	3.6	3.7	
SD	0.4	0.3	
Creatinine, mg/dL			.931
Mean	0.72	0.70	
SD	0.25	0.17	
AST, U/L			430
Mean	37	29	
SD	26	13	
ALT, U/L			.624
Mean	43	32	
SD	37	24	
ALP, U/L			.815
Mean	593	459	
SD	591	283	
Pharmacokinetic parameters of gemcitabine			
C_{max}, μg/mL			.594
Mean	24.02	23.21	
SD	7.18	6.68	
AUC, h · μg/mL			.462
Mean	9.95	10.74	
SD	2.36	3.03	

NOTE. Kruskal-Wallis test was applied to assess differences of values.
Abbreviations: AE, adverse event; SD, standard deviation; ECOG, Eastern Cooperative Oncology Group; FU, fluorouracil; LAPC, locally advanced pancreatic cancer; ALP, alkaline phosphatase; C_{max}, peak concentration; AUC, area under the curve.
*Calculated using the χ^2 test.

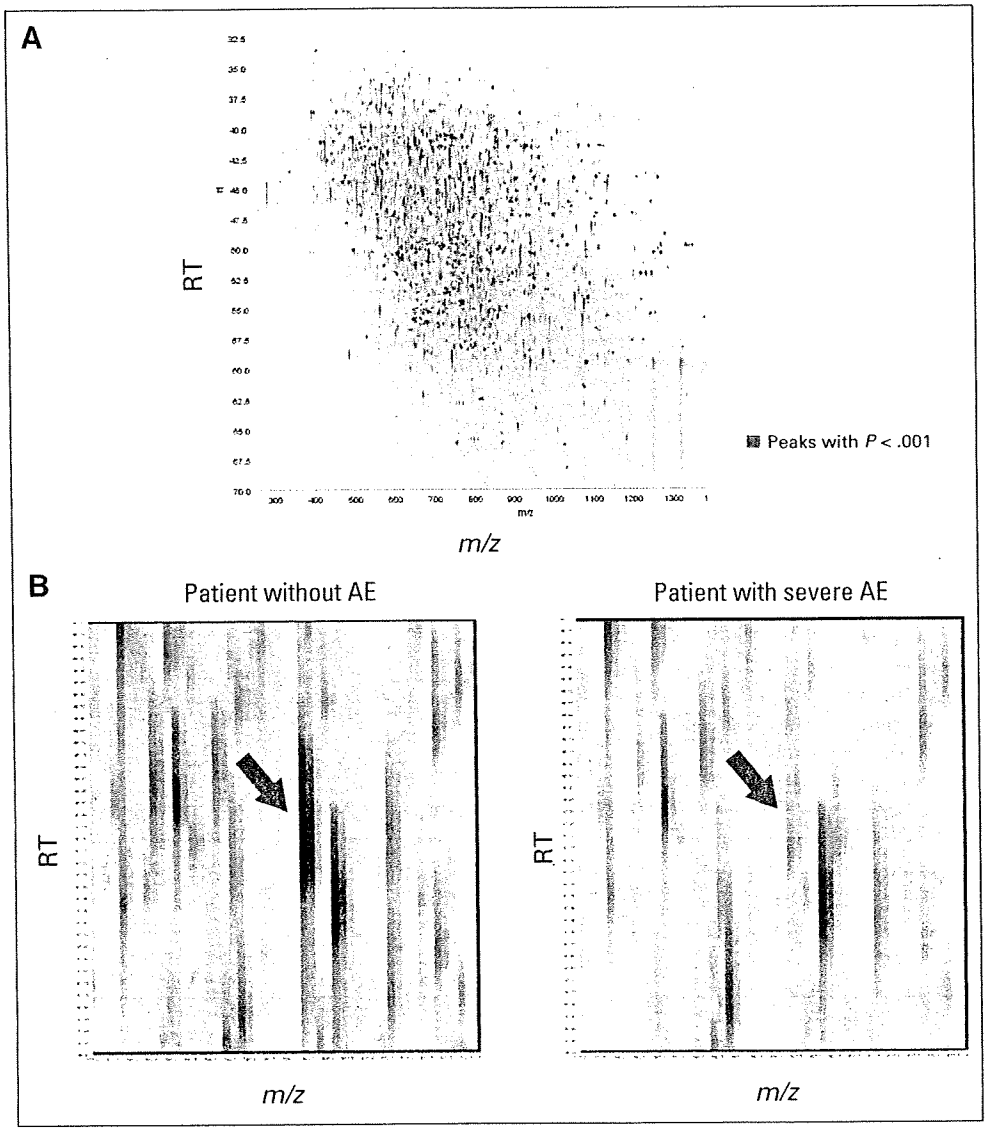

Fig 1. (A) Two-dimensional display of the entire (> 60,000) mass spectrometry (MS) peaks. The 757 MS peaks whose mean intensity differed significantly between patients with severe adverse events (AEs) and patients without AEs ($P < .001$, Welch t test) are highlighted in red. (B) MS peak with the smallest P value ($P = .0000282$; red arrows) in representative patients with severe AEs (right) and without AEs (left). RT, retention time.

two independent validation cohorts V1 (Fig 3B and Appendix Table A2) and V2 (Fig 3C and Appendix Table A3). The correlations between the levels of haptoglobin and the toxicity categories showed the highest statistical significance in all three cohorts (Figs 3A to 3C). The toxicity categories are criteria that we devised to evaluate the clinical severity of overall hematologic toxicities with emphasis on thrombocytopenia (Appendix Fig A1) from a practical viewpoint.[26-28] The management of neutropenia is largely uncomplicated because of the availability of granulocyte colony-stimulating factor.

Haptoglobin Phenotype and Hematologic Toxicities

Haptoglobin is a plasma protein that binds free hemoglobin and inhibits its oxidative activity. The human *HP* gene has two common polymorphic alleles (*H1* and *H2*), yielding individuals with the following three distinct phenotypes in the α-chain of haptoglobin protein: Hp 1-1, Hp 2-1, and Hp 2-2. The *H2* genotype has been reported to be associated with an increased risk of myocardial infarction and juvenile diabetes.[29] Although the frequency of the three phenotypes did not differ significantly with the severity of hematologic toxicities ($P > .360$, χ^2 test; Table 1 and Appendix Tables A1 to A3), the levels of haptoglobin were lower in individuals with the Hp 2-2 phenotype than in those with the Hp 2-1 or Hp 1-1 phenotype (Appendix Fig A3, online only).

Construction and Validation of a Model Predicting Hematologic Toxicities

In the M0 cohort (n = 166), 68 patients (41%) experienced category III hematologic toxicities, and 18 patients (11%) experienced category IV hematologic toxicities. Such levels of AE often necessitate the postponement of chemotherapy, and therefore, their prediction before drug administration is desirable. Because none of the parameters, including haptoglobin, was able to predict AEs satisfactorily when used individually (data not shown), we attempted to construct a multivariate predictive model to estimate the relative risk of suffering from hematologic toxicities of category III or worse. We searched for these parameters using a forward stepwise selection procedure by AIC

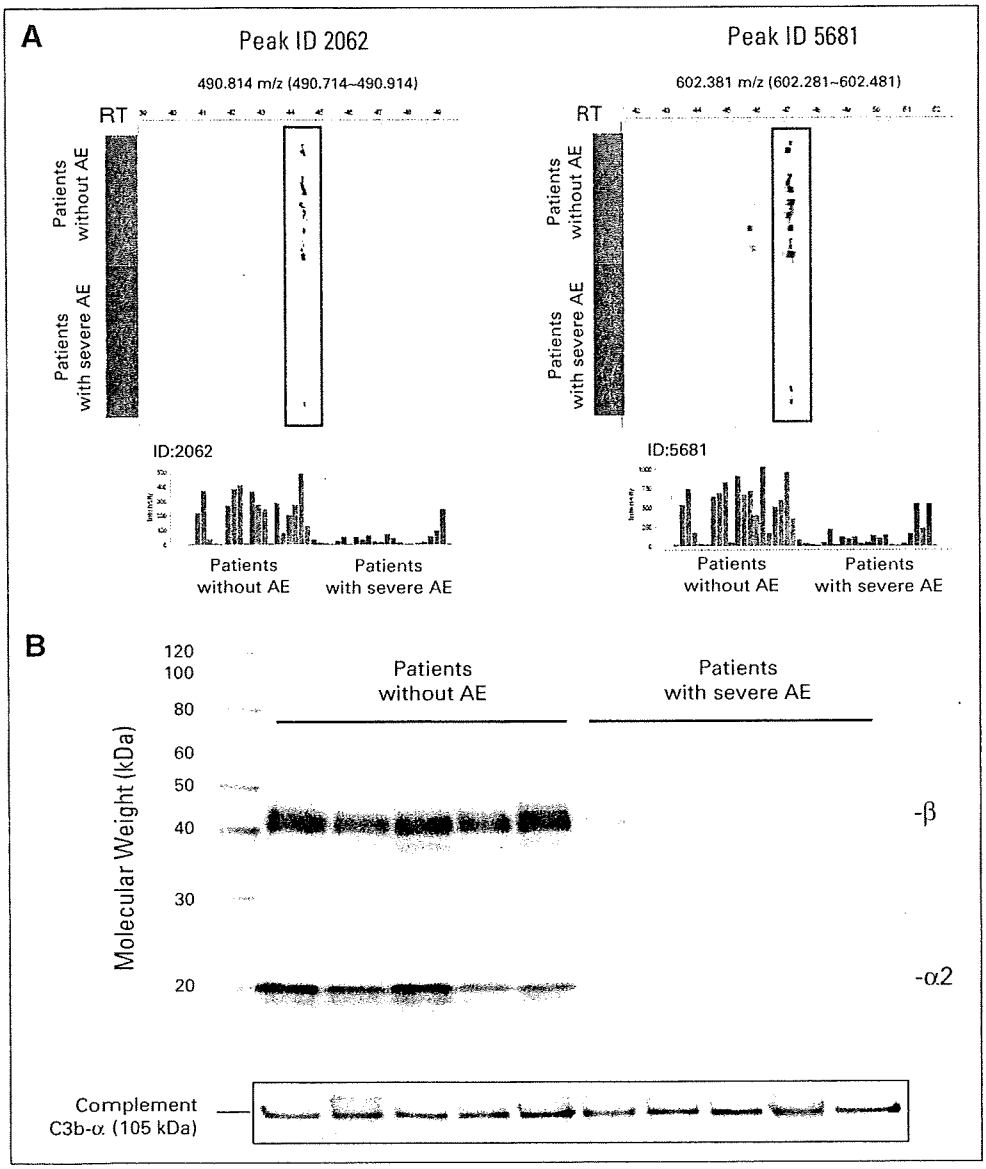

Fig 2. (A) Representative haptoglobin-derived mass spectrometry (MS) peaks in 47 triplicate liquid chromatography (LC)/MS runs (22 without adverse events [AEs], blue; and 25 with severe AEs, red) aligned along the retention time (RT) of LC (top). Columns represent the mean intensity of triplicates (bottom). (B) Detection of β- and α2-chains of haptoglobin and complement C3b-α (loading control) by immunoblotting.

from all of the clinical and laboratory data listed in Appendix Table A1 (available for 162 patients) and found that a combination of plasma haptoglobin level, haptoglobin phenotype, absolute neutrophil count (ANC), platelet count, and body-surface area (BSA) provided the lowest AIC value. The prediction model using this combination of parameters was significantly compromised when haptoglobin level and phenotype were excluded ($\chi^2 = 11.49, df = 3, P = .009$, likelihood ratio test). We estimated the independent contribution of each parameter to this prediction model and found that the baseline haptoglobin level was the second most important contributor to the model (Table 2).

On the basis of the results of multivariate logistic regression analysis, we constructed a nomogram in which the values of the five parameters (haptoglobin level, haptoglobin phenotype, ANC, platelet count, and BSA) are integrated into a single score (total point) to estimate the relative risk of having hematologic toxicities more severe than category II, category III, or category IV (Fig 4A). The area under the curve value for the prediction of categories III to IV was calculated to be 0.782 (95% CI, 0.711 to 0.843) in cohort M0 (Fig 4B). Predictive ability was confirmed in two independent validation cohorts, V1 and V2, that were not used for construction of the nomogram, with area under the curve values of 0.655 (95% CI, 0.546 to 0.754) and 0.747 (95% CI, 0.606 to 0.858), respectively (Fig 4B).

DISCUSSION

The early onset of severe AE necessitates dose reduction or postponement of treatment, leading to failure of chemotherapy.[30,31] In particular, the current gemcitabine monotherapy against advanced pancreatic cancer is mainly aimed at disease palliation, and thus, avoidance of life-threatening AEs is necessary. In this study, we first compared the plasma proteome of two groups of patients who showed distinct responses to the same protocol of gemcitabine therapy (Fig 1).

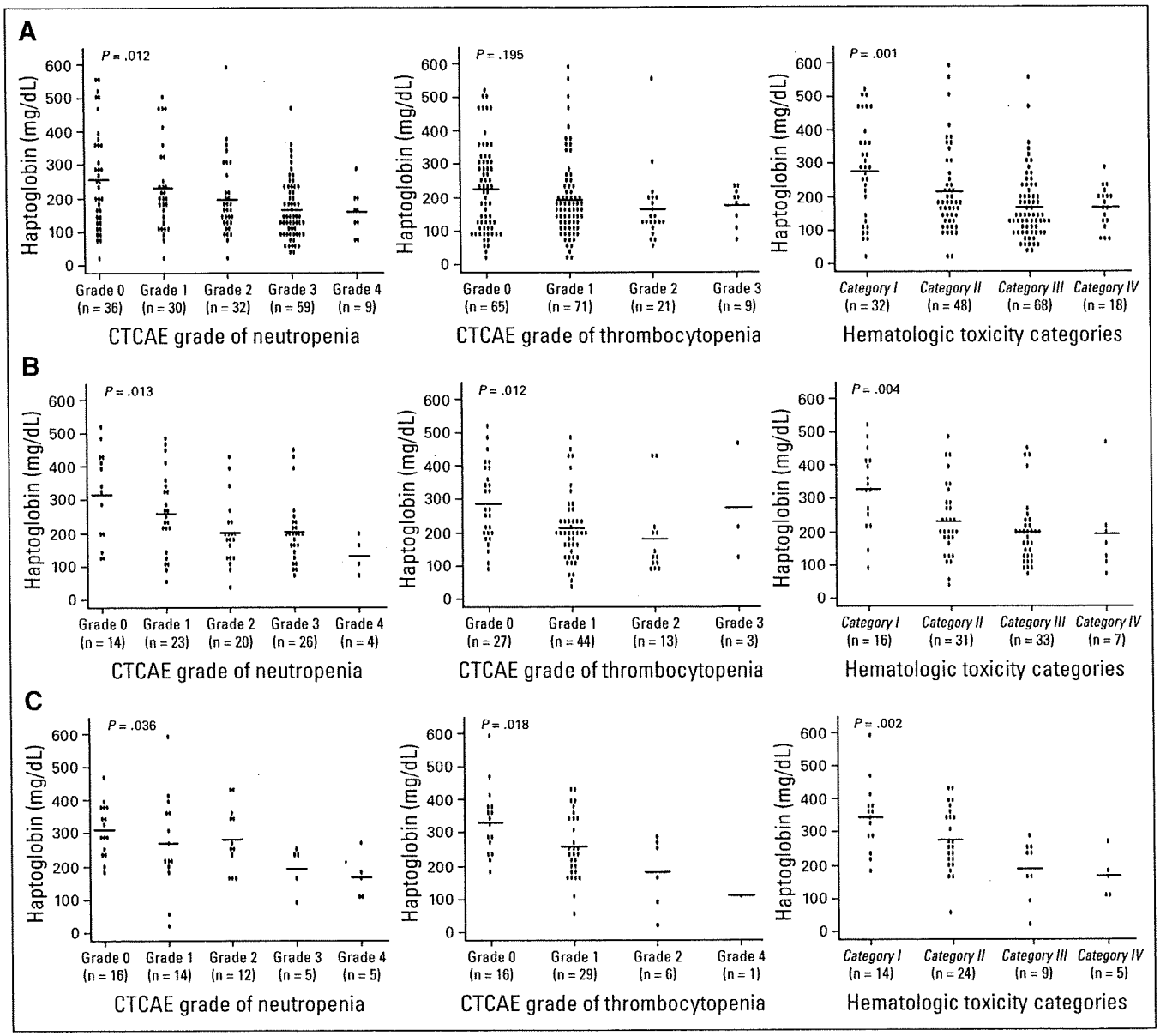

Fig 3. Plasma/serum haptoglobin levels according to the Common Terminology Criteria of Adverse Events (CTCAE; version 3.0). Grades of neutropenia (left), thrombocytopenia (middle), and hematologic toxicity categories (right) in the (A) modeling (M0), (B) validation-1 (V1), and (C) validation-2 (V2) cohorts. Horizontal lines represent the average levels of haptoglobin.

There was no significant difference in age distribution, Eastern Cooperative Oncology Group performance status, liver function, renal function, or prior chemoradiotherapy between the groups (Table 1 and data not shown), indicating that the occurrence of AEs does not merely reflect the general poor condition of patients but is based on certain biologic differences among individuals. We found that individuals who experienced severe AEs after administration of gemcitabine showed decreased baseline levels of plasma haptoglobin (Figs 1B and 2A), and this result was validated in three large cohorts using a different methodology (Fig 3 and Appendix Tables A1 to A3). Haptoglobin is an abundant plasma protein that usually cannot be measured by direct MS. However, constant depletion using an IgY-12 High Capacity Spin Column[32] allowed us to accentuate the differences in haptoglobin levels.

The molecular mechanisms that regulate the plasma haptoglobin level under physiologic and pathologic conditions are largely unknown. Haptoglobin is produced mainly in the liver, taken up by neutrophils, and stored within their cytoplasmic granules. Haptoglobin is released in response to a variety of stimuli, such as infection, trauma, and malignancy,[33] and modulates inflammatory responses. Tumor necrosis factor α induces the release of haptoglobin from neutrophils in vitro.[34] Interestingly, tumor necrosis factor α and its soluble receptors have been reported to be associated with an increased risk of hematologic toxicities.[12,35,36]

Table 2. Contribution of Parameters to Prediction of Hematologic Toxicities Associated With Gemcitabine

Factor	Odds Ratio*	95% CI	P
Haptoglobin level	0.71	0.53 to 0.97	.031†
Phenotype of haptoglobin (v Hp 2-2)			
Hp 2-1	0.61	0.31 to 1.21	.159
Hp 1-1	2.16	0.70 to 6.69	.180
Absolute neutrophil count	0.72	0.61 to 0.86	.0003†
Platelet count	0.63	0.39 to 1.01	.056
Body-surface area	3.86	0.63 to 23.76	.145

NOTE. A forward stepwise selection based on Akaike's Information Criterion was used to select parameters for multivariate analysis.
*Odds ratios are per 100 mg/dL increase for haptoglobin level, per 1,000/μL increase for absolute neutrophil count, per 10×10^4/μL increase for platelet, and per 1.00 m^2 increase for body-surface area.
†$P < .05$.

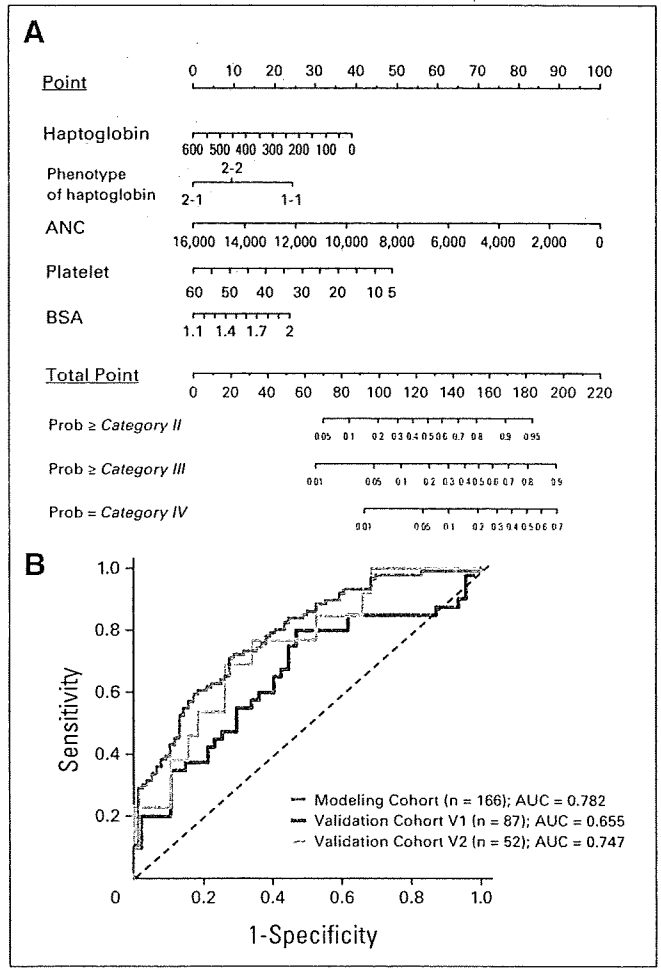

Fig 4. (A) Nomogram to estimate the risk of hematologic toxicities more severe than category II (top), category III (middle), and category IV (bottom). Please see Appendix Figure A4 and its legend for usage. (B) Receiver operating characteristic (ROC) analysis of nomogram for the prediction of category III and IV hematologic toxicities in the modeling (gray), validation-1 (V1; blue), and validation-2 (V2; gold) cohorts. ANC, absolute neutrophil count; BSA, body-surface area; AUC, area under the curve.

To derive clinical applicability from these basic findings, we constructed a model (nomogram) that estimates the possibility of occurrence of hematologic AE before administration of gemcitabine (Fig 4A and Appendix Fig A4). The significance of the model was further confirmed in two independent validation cohorts (Fig 4B). Although its accuracy was far from perfect, the model seems to be practically sufficient for identifying individuals who are likely to suffer from hematologic toxicities after administration of gemcitabine. Various cytotoxic or molecular targeting agents have been tested in combination with gemcitabine in phase III trials, but no apparent additional therapeutic benefit has been demonstrated.[5,6,9,10] The application of this model to patient selection may improve the outcome of such trials. We are now trying to identify new biomarkers that can predict the efficacy of gemcitabine treatment using a similar strategy.

The phenotypes of haptoglobin have been reported to be associated with different hemoglobin-binding, antioxidative, and prostaglandin synthesis–initiating activities.[33] Although haptoglobin phenotype was not significantly associated with hematologic toxicities (Table 1 and Appendix Tables A1 to A3), the average levels of haptoglobin differed among individuals with different phenotypes (Appendix Fig A3), as described previously.[33] For this reason, haptoglobin phenotype was selected in the prediction model by AIC analysis (Table 2). BSA has been repeatedly selected as one of the multivariate parameters for predicting the AEs of anticancer therapies in other studies,[14,37] suggesting a potential lack of accuracy in calculating individually optimized drug dose based solely on BSA, as pointed out previously.[38,39]

In conclusion, we have revealed that a decreased level of haptoglobin is the second most significant factor predicting hematologic toxicities associated with gemcitabine monotherapy after ANC (Table 2). Measurement of haptoglobin is now established as a laboratory test and could be readily incorporated into routine oncologic practice. However, the predictive significance of haptoglobin was revealed only in a retrospective population from a single institution and must, therefore, be validated in an independent prospective multi-institutional study. It was not determined in this study whether haptoglobin could be a predictive biomarker for the AEs of other chemotherapeutic agents. To improve the accuracy of prediction, the discovery of new biomarkers with higher specificity and sensitivity will be necessary. While bearing all these limitations in mind, the present findings may provide novel insights not only into the molecular mechanisms by which gemcitabine causes hematologic toxicities, but also into new avenues for the development of new chemotherapeutic agents with lower toxicity.

AUTHORS' DISCLOSURES OF POTENTIAL CONFLICTS OF INTEREST

Although all authors completed the disclosure declaration, the following author(s) indicated a financial or other interest that is relevant to the subject matter under consideration in this article. Certain relationships marked with a "U" are those for which no compensation was received; those relationships marked with a "C" were compensated. For a detailed description of the disclosure categories, or for more information about ASCO's conflict of interest policy, please refer to the Author Disclosure Declaration and the Disclosures of Potential Conflicts of Interest section in Information for Contributors.

Employment or Leadership Position: None **Consultant or Advisory Role:** None **Stock Ownership:** None **Honoraria:** Nagahiro Saijo, Elli

Lilly **Research Funding:** Nagahiro Saijo, National Institute of Biomedical Innovation **Expert Testimony:** None **Other Remuneration:** None

AUTHOR CONTRIBUTIONS

Conception and design: Junichi Matsubara, Masaya Ono, Setsuo Hirohashi, Tesshi Yamada
Financial support: Nagahiro Saijo, Tesshi Yamada
Administrative support: Tsutomu Chiba, Setsuo Hirohashi
Provision of study materials or patients: Hideki Ueno, Takuji Okusaka, Junji Furuse, Koh Furuta, Emiko Sugiyama, Yoshiro Saito, Nahoko Kaniwa, Junichi Sawada
Collection and assembly of data: Junichi Matsubara, Ayako Negishi, Kazufumi Honda, Nagahiro Saijo, Tesshi Yamada
Data analysis and interpretation: Junichi Matsubara, Masaya Ono, Tomohiro Sakuma
Manuscript writing: Junichi Matsubara, Tesshi Yamada
Final approval of manuscript: Junichi Matsubara, Masaya Ono, Junichi Sawada, Tsutomu Chiba, Nagahiro Saijo, Setsuo Hirohashi, Tesshi Yamada

REFERENCES

1. Honda K, Hayashida Y, Umaki T, et al: Possible detection of pancreatic cancer by plasma protein profiling. Cancer Res 65:10613-10622, 2005
2. Ministry of Health, Labour and Welfare: Japanese Government: Statistical Database 2007. http://wwwdbtk.mhlw.go.jp/toukei/youran/data19k/1-31.xls
3. American Cancer Society: Cancer Facts and Figures 2007. Atlanta, GA: American Cancer Society, 2007
4. Burris HA 3rd, Moore MJ, Andersen J, et al: Improvements in survival and clinical benefit with gemcitabine as first-line therapy for patients with advanced pancreas cancer: A randomized trial. J Clin Oncol 15:2403-2413, 1997
5. Louvet C, Labianca R, Hammel P, et al: Gemcitabine in combination with oxaliplatin compared with gemcitabine alone in locally advanced or metastatic pancreatic cancer: Results of a GERCOR and GISCAD phase III trial. J Clin Oncol 23:3509-3516, 2005
6. Herrmann R, Bodoky G, Ruhstaller T, et al: Gemcitabine plus capecitabine compared with gemcitabine alone in advanced pancreatic cancer: A randomized, multicenter, phase III trial of the Swiss Group for Clinical Cancer Research and the Central European Cooperative Oncology Group. J Clin Oncol 25:2212-2217, 2007
7. National Comprehensive Cancer Network: Clinical Practice Guidelines in Oncology: Pancreatic Adenocarcinoma V. 1. 2008. http://www.nccn.org/professionals/physician_gls/PDF/pancreatic.pdf
8. Casper ES, Green MR, Kelsen DP, et al: Phase II trial of gemcitabine (2,2'-difluorodeoxycytidine) in patients with adenocarcinoma of the pancreas. Invest New Drugs 12:29-34, 1994
9. Kindler HL, Niedzwiecki D, Hollis D, et al: A double-blind, placebo-controlled, randomized phase III trial of gemcitabine (G) plus bevacizumab (B) versus gemcitabine plus placebo (P) in patients (pts) with advanced pancreatic cancer (PC): A preliminary analysis of Cancer and Leukemia Group B (CALGB). J Clin Oncol 25:199s, 2007 (suppl; abstr 4508)
10. Philip PA, Benedetti J, Fenoglio-Preiser C, et al: Phase III study of gemcitabine (G) plus cetuximab versus gemcitabine (C) in patients (pts) with locally advanced or metastatic pancreatic adenocarcinoma (Pca): SWOG S0205 study. J Clin Oncol 25:199s, 2007 (suppl; abstr LBA4509)
11. Ziepert M, Schmits R, Trumper L, et al: Prognostic factors for hematotoxicity of chemotherapy in aggressive non-Hodgkin's lymphoma. Ann Oncol 19:752-762, 2008
12. Voog E, Bienvenu J, Warzocha K, et al: Factors that predict chemotherapy-induced myelosuppression in lymphoma patients: Role of the tumor necrosis factor ligand-receptor system. J Clin Oncol 18:325-331, 2000
13. Pond GR, Siu LL, Moore M, et al: Nomograms to predict serious adverse events in phase II clinical trials of molecularly targeted agents. J Clin Oncol 26:1324-1330, 2008
14. Aslani A, Smith RC, Allen BJ, et al: The predictive value of body protein for chemotherapy-induced toxicity. Cancer 88:796-803, 2000
15. Sugiyama E, Kaniwa N, Kim SR, et al: Pharmacokinetics of gemcitabine in Japanese cancer patients: The impact of a cytidine deaminase polymorphism. J Clin Oncol 25:32-42, 2007
16. Yonemori K, Ueno H, Okusaka T, et al: Severe drug toxicity associated with a single-nucleotide polymorphism of the cytidine deaminase gene in a Japanese cancer patient treated with gemcitabine plus cisplatin. Clin Cancer Res 11:2620-2624, 2005
17. Hanash S: Disease proteomics. Nature 422: 226-232, 2003
18. Yamaguchi U, Nakayama R, Honda K, et al: Distinct gene expression-defined classes of gastrointestinal stromal tumor. J Clin Oncol 26:4100-4108, 2008
19. Taguchi F, Solomon B, Gregorc V, et al: Mass spectrometry to classify non-small-cell lung cancer patients for clinical outcome after treatment with epidermal growth factor receptor tyrosine kinase inhibitors: A multicohort cross-institutional study. J Natl Cancer Inst 99:838-846, 2007
20. Yanagisawa K, Tomida S, Shimada Y, et al: A 25-signal proteomic signature and outcome for patients with resected non-small-cell lung cancer. J Natl Cancer Inst 99:858-867, 2007
21. Ono M, Shitashige M, Honda K, et al: Label-free quantitative proteomics using large peptide data sets generated by nanoflow liquid chromatography and mass spectrometry. Mol Cell Proteomics 5:1338-1347, 2006
22. General Rules for the Study of Pancreatic Cancer (ed 5). Tokyo, Japan Japanese Pancreas Society
23. Honda K, Yamada T, Hayashida Y, et al: Actinin-4 increases cell motility and promotes lymph node metastasis of colorectal cancer. Gastroenterology 128:51-62, 2005
24. Idogawa M, Yamada T, Honda K, et al: Poly(ADP-ribose) polymerase-1 is a component of the oncogenic T-cell factor-4/beta-catenin complex. Gastroenterology 128:1919-1936, 2005
25. Tolson J, Bogumil R, Brunst E, et al: Serum protein profiling by SELDI mass spectrometry: Detection of multiple variants of serum amyloid alpha in renal cancer patients. Lab Invest 84:845-856, 2004
26. Tempero M, Plunkett W, Ruiz Van Haperen V, et al: Randomized phase II comparison of dose-intense gemcitabine: Thirty-minute infusion and fixed dose rate infusion in patients with pancreatic adenocarcinoma. J Clin Oncol 21:3402-3408, 2003
27. Kindler HL, Friberg G, Singh DA, et al: Phase II trial of bevacizumab plus gemcitabine in patients with advanced pancreatic cancer. J Clin Oncol 23: 8033-8040, 2005
28. Cascinu S, Berardi R, Labianca R, et al: Cetuximab plus gemcitabine and cisplatin compared with gemcitabine and cisplatin alone in patients with advanced pancreatic cancer: A randomised, multicentre, phase II trial. Lancet Oncol 9:39-44, 2008
29. Shindo S: Haptoglobin subtyping with anti-haptoglobin alpha chain antibodies. Electrophoresis 11:483-488, 1990
30. Hryniuk W, Bush H: The importance of dose intensity in chemotherapy of metastatic breast cancer. J Clin Oncol 2:1281-1288, 1984
31. Levin L, Hryniuk WM: Dose intensity analysis of chemotherapy regimens in ovarian carcinoma. J Clin Oncol 5:756-767, 1987
32. Huang L, Harvie G, Feitelson JS, et al: Immunoaffinity separation of plasma proteins by IgY microbeads: Meeting the needs of proteomic sample preparation and analysis. Proteomics 5:3314-3328, 2005
33. Langlois MR, Delanghe JR: Biological and clinical significance of haptoglobin polymorphism in humans. Clin Chem 42:1589-1600, 1996
34. Berkova N, Gilbert C, Goupil S, et al: TNF-induced haptoglobin release from human neutrophils: Pivotal role of the TNF p55 receptor. J Immunol 162:6226-6232, 1999
35. Petros WP, Rabinowitz J, Gibbs JP, et al: Effect of plasma TNF-alpha on filgrastim-stimulated hematopoiesis in mice and humans. Pharmacotherapy 18:816-823, 1998
36. Holler E, Kolb HJ, Moller A, et al: Increased serum levels of tumor necrosis factor alpha precede major complications of bone marrow transplantation. Blood 75:1011-1016, 1990
37. Shayne M, Culakova E, Poniewierski MS, et al: Dose intensity and hematologic toxicity in older cancer patients receiving systemic chemotherapy. Cancer 110:1611-1620, 2007
38. Ratain MJ: Body-surface area as a basis for dosing of anticancer agents: Science, myth, or habit? J Clin Oncol 16:2297-2298, 1998
39. Gurney H: Dose calculation of anticancer drugs: A review of the current practice and introduction of an alternative. J Clin Oncol 14:2590-2611, 1996

Acknowledgment

We thank Ayako Igarashi and Yuka Nakamura for their technical assistance.

SHOCK, Vol. 31, No. 4, pp. 397–403, 2009

DOES PROLONGED BILIARY OBSTRUCTIVE JAUNDICE SENSITIZE THE LIVER TO ENDOTOXEMIA?

Ayako Iida, Hiroyuki Yoshidome, Takashi Shida, Fumio Kimura, Hiroaki Shimizu, Masayuki Ohtsuka, Yasuhiro Morita, Dan Takeuchi, and Masaru Miyazaki

Department of General Surgery, Chiba University Graduate School of Medicine, Chiba, Japan

Received 21 Apr 2008; first review completed 05 May 2008; accepted in final form 10 Jun 2008

ABSTRACT—Biliary obstructive jaundice (OJ) is an important clinical consideration concerning high bacteremic risk. Hepatocyte apoptosis is one of the causes of cholestatic liver injury. The aim of the current study was to examine the precise pathway and time course of hepatocyte apoptosis during OJ with LPS administration and to determine if OJ sensitizes the liver to endotoxemia. Male C57BL/6 mice were subjected to bile duct ligation and division and were administered with LPS at 3 (OJ3) or 14 (OJ14) days after surgery. Fas ligand expression, poly (adenosine diphosphate–ribose) polymerase p85 fragment immunohistochemistry, activation of caspases 3, 8, and 9, serum alanine aminotransferase levels, and hepatic adenosine triphosphate (ATP) contents were examined. Survival after LPS administration in male C57BL/6 or gld/gld (Fas ligand–deficient) mice was determined. The expression of Fas ligand increased during OJ. After LPS administration, the expression of cleaved caspases 3 and 8 increased in Sham3, Sham14, OJ3, and OJ14 mice, and it significantly increased in OJ14 compared with other mice. Poly (adenosine diphosphate–ribose) polymerase p85 immunohistochemistry showed significant hepatocyte apoptosis after LPS administration in OJ14 mice relative to OJ3. In OJ14 with LPS administration, ATP contents significantly decreased and alanine aminotransferase levels increased. Hepatocyte apoptosis was decreased in gld/gld OJ14 mice compared with C57BL/6 OJ14. All C57BL/6 OJ14 mice with LPS died, but survival in gld/gld OJ14 significantly ameliorated. In prolonged OJ with LPS administration, hepatocyte apoptosis depending on Fas ligand expression significantly increased in association with a decrease in ATP contents, thus resulting in liver necrapoptosis.

KEYWORDS—Apoptosis, liver failure, transcription factor, death signal, Fas ligand

ABBREVIATIONS—ALT–alanine aminotransferase; ELISA–enzyme-linked immunosorbent assay; OJ–obstructive jaundice; PARP–poly (adenosine diphosphate–ribose) polymerase; T-BIL–total bilirubin

INTRODUCTION

Biliary obstructive jaundice (OJ) due to malignancy of the biliary tract or biliary inflammation is associated with liver dysfunction and susceptibility to infection (1–3). Biliary infection concomitant with biliary obstruction, which raises the intraductal pressure in the bile duct, may cause cholangitis due to either cholangiovenous or cholangiolymphatic reflux (4). In addition, the presence of OJ has been reported to increase the postoperative bacteremic risk, and performance of extended hepatectomy increased the risk, suggesting that when patients having biliary carcinoma with OJ undergo extended hepatectomy, risk of infectious complication significantly increased (5). Belghiti et al. (6) also analyzed operative risks and showed that the mortality of patients with OJ was extremely high (21%) as compared with that of patients with a normal liver function. Therefore, in clinical settings, association between OJ, infection, and liver dysfunction needs to be clarified.

In OJ, bile acids accumulate to cause hepatocyte apoptosis, which has been shown to be involved in Fas (7, 8). Fas ligand (FasL) and TNF-α–associated death domains promote binding of procaspase 8 and subsequent proteolytic activation of catalytic caspase 8, which is known as the type 1 signaling pathway. Caspase 8 is able to directly activate caspase 3, which is an executioner caspase, leading to apoptosis (9). Conversely, the type 2 signaling pathway is the onset of the mitochondrial permeability transition, leading to cytochrome *c* release (10). The cytochrome *c* complex proteolytically activates caspase 9, and subsequently activates caspase 3 (11). Although the occurrence of hepatocyte apoptosis has been shown in OJ, the time course of activation of caspases and the precise mechanism leading to hepatocyte apoptosis during OJ and OJ with LPS administration have not yet been thoroughly elucidated. Furthermore, in models of liver injury, hepatocytes often show the morphological features of apoptosis and necrosis, for which the term "necrapoptosis" has been coined (12). There seems to be several cellular determinants that shift the balance from one pathway to the other. Apoptosis requires adenosine triphosphate (ATP), and a switch from apoptosis to necrosis occurs when cells are devoid of ATP (12). The aim of the current study was to determine whether hepatocyte apoptosis with subsequent liver injury during OJ is augmented after LPS administration and to determine the precise pathway leading to apoptosis/necrapoptosis. The present study investigated the expression of caspase 3, 8, and 9, immunohistochemistry of poly (adenosine diphosphate–ribose) polymerase (PARP) p85 fragment, hepatic ATP contents, histology, liver injury, and survival in the short and prolonged periods of OJ with LPS administration.

Address reprint requests to Hiroyuki Yoshidome, MD, Department of General Surgery, Chiba University Graduate School of Medicine, 1-8-1 Inohana Chuo-ku Chiba 260-0856, Japan. E-mail: h-yoshidome@faculty.chiba-u.jp.

This study was supported in part by the Japan Society for the Promotion of Science (grant no. 19591577).

DOI: 10.1097/SHK.0b013e31818349ea

MATERIALS AND METHODS

Male C57BL/6 or gld/gld (FasL-deficient) mice (Japan SLC, Inc. Hamamatsu, Japan) weighing 22 to 27 g were housed in a controlled environment, exposed to a 12-h light/dark cycle, and provided with commercial chow and water *ad libitum*. This project was approved by Chiba University Animal Care and Use committee and was in compliance with the National Institutes of Health guidelines.

Bile duct ligation and LPS administration model

The cholestatic mouse model was used; male C57BL/6 or gld/gld mice were anesthetized with sodium pentobarbital (60 mg/kg, administered i.p.), and the common bile duct was isolated after laparotomy. The common bile duct was ligated at three sites and divided between the proximal double and the distal single ligation. Sham-operated mice underwent the same procedure without bile duct ligation and division. At 3 or 14 days after sham surgery or bile duct ligation and division, jaundiced or sham-operated mice were anesthetized with sodium pentobarbital and LPS (4 mg/kg; *Escherichia coli*; Sigma Aldrich, St. Louis, Mo) in 0.1 mL sterile saline, or sterile saline (0.1 mL) was injected via the lateral tail vein. Mice were killed at 3 h after LPS or sterile saline administration, and liver tissue and blood samples were taken for analysis. Survival was also examined after LPS administration.

Analysis of apoptosis and histological examination

Liver tissue specimens were obtained, and sections of formalin-fixed, paraffin-embedded liver samples were stained with hematoxylin-eosin to assess the degree of liver injury. To evaluate hepatocyte apoptosis, immunohistochemistry was performed for PARP p85 fragment, which is cleaved by caspase 3 from PARP (116 kd; Promega, Madison, Wis; original magnification, 200×). To calculate the apoptotic index of PARP p85 fragment, the number of stained and unstained hepatocytes was counted in five random fields (400×). Comparative staining with Meyer hematoxylin was also performed.

Western blot analysis

Liver tissue specimens were obtained and immediately frozen in liquid nitrogen. Frozen liver specimens were homogenized in lysis buffer (10 mM HEPES [pH 7.9], 150 mM NaCl, 1 mM ethylenediaminetetraacetic acid, 0.6% NP-40, 0.5 mM phenylmethylsulfonyl fluoride, 1 μg/mL leupeptin, 1 μg/mL aprotinin, 10 μg/mL soybean trypsin inhibitor, and 1 μg/mL pepstatin) on ice. The homogenates were sonicated and centrifuged at 5,000 rpm to remove cellular debris. The total protein concentration of each sample was measured by a bicinchoninic assay kit using bovine serum albumin as a reference standard (Pierce Chemical Co. Rockford, Ill). Liver lysates were subjected to

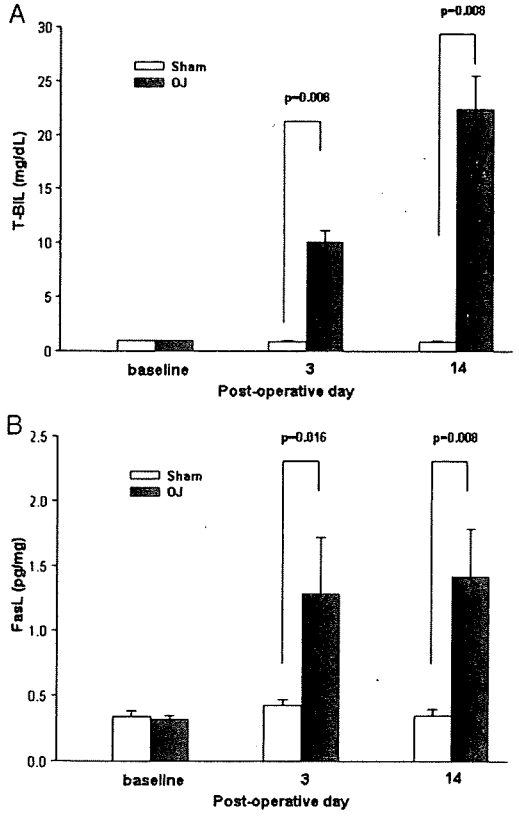

FIG. 1. **A, Serum T-BIL levels were analyzed.** B, The protein expression of FasL was analyzed by tissue ELISA. Samples were obtained from the normal, Sham3, Sham14, OJ3, and OJ14 mice. Data are mean ± SEM. No significant difference was observed in the T-BIL levels or the FasL expression among the normal (baseline), Sham3, and Sham14 mice. For all groups, n = 5.

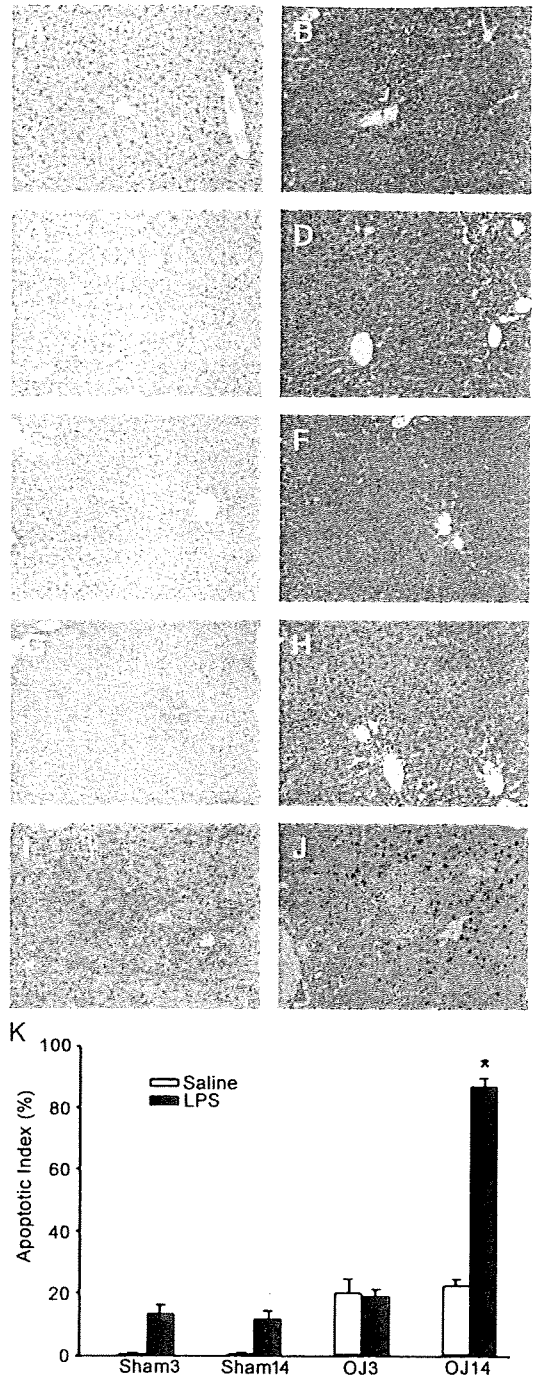

FIG. 2. **Hepatic apoptosis and histological findings after LPS administration.** Apoptosis was assessed by PARP p85 fragment immunohistochemistry (A, C, E, G, and I; original magnification, 200×). Liver histopathology was evaluated by hematoxylin-eosin staining (B, D, F, H, and J; original magnification, 200×). Liver tissue obtained from sham-operated mice at 3 h after saline administration (A and B) and Sham3 (C and D), Sham14 (E and F), OJ3 (G and H), and OJ14 (I and J) at 3 h after LPS administration. K, Apoptotic index of PARP p85. To calculate the apoptotic index, the number of stained and unstained hepatocytes was counted in five random fields (original magnification, 400×). Data are mean ± SEM. $^*P < 0.001$ vs. other mice. For all groups, n = 6.

the XV PANTERA system (DRC, Tokyo, Japan). Samples were electrophoresed in a precast 15% XV PANTERA gel and transferred to a polyvinylidene difluoride membrane. Nonspecific binding sites were blocked with Tris-buffered saline (TBS; 40 mM Tris [pH 7.6] and 300 mM NaCl) with 0.1% Tween 20 containing 5% nonfat dry milk for 1 h at room temperature. Membranes were then incubated with antibodies to rabbit polyclonal antimouse actin, caspases 3, 8, and 9 (Santa Cruz Biotechnology, Santa Cruz, Calif), in TBS Tween 20. After five washes in TBS Tween 20, the membranes were incubated with horseradish peroxidase–conjugated donkey antirabbit immunoglobulin G. The immunoreactive proteins were detected by enhanced chemiluminescence according to the manufacturer's instructions, and the quantification data were analyzed with the image analysis software program (National Institutes of Health image, Bethesda, Md).

Blood and tissue analysis

Blood was obtained by cardiac puncture at the time of killing. Serum samples were analyzed for alanine aminotransferase (ALT) as indices of hepatocellular injury and serum total bilirubin (T-BIL) concentrations using a diagnostic kit (WAKO Pure Chemical Industries, Osaka, Japan). A quantitative assessment of FasL in the liver was made as described elsewhere (13). Briefly, liver tissue specimens were obtained and were immediately frozen. Frozen liver tissue was homogenized in 10 volumes of homogenization buffer (10 mM ethylenediaminetetraacetic acid, 2 mM phenylmethylsulfonyl fluoride, 0.1 mg/mL soybean trypsin inhibitor, 1.0 mg/mL bovine serum albumin, 0.02% sodium azide, and 0.2 μl/mL protease inhibitor cocktail [1,000 × stock; 1 mg/mL leupeptin, 1 mg/mL aprotinin, and 1 mg/mL pepstatin]). After incubating for 2 h at 4°C, the homogenate was centrifuged at 12,500 × *g* for 10 min. The supernatant was removed and centrifuged again to obtain a clear lysate. Total protein concentration of each sample was determined as described for Western blot, and samples were dispensed for enzyme-linked immunosorbent assay (ELISA) for the assessment of FasL according to the manufacturer's instructions (R&D Systems, Inc., Minneapolis, Minn). The concentration was calculated per mg total protein.

Hepatic ATP content

Liver tissue specimens were obtained and were immediately frozen. Adenosine triphosphate concentrations present in whole liver lysates were determined by using the Firefly luciferase ATP determination kit (Invitrogen, Carlsbad, Calif). Samples were prepared according to the manufacturer's instructions. Luminescence was determined using a luminometer (Berthold Technologies, Bad Wildbad, Germany), and values were calculated based on an ATP standard curve.

Statistical analysis

All data are expressed as the mean ± SEM. Comparisons between two groups were analyzed using a Mann-Whitney *U* test. Comparisons between

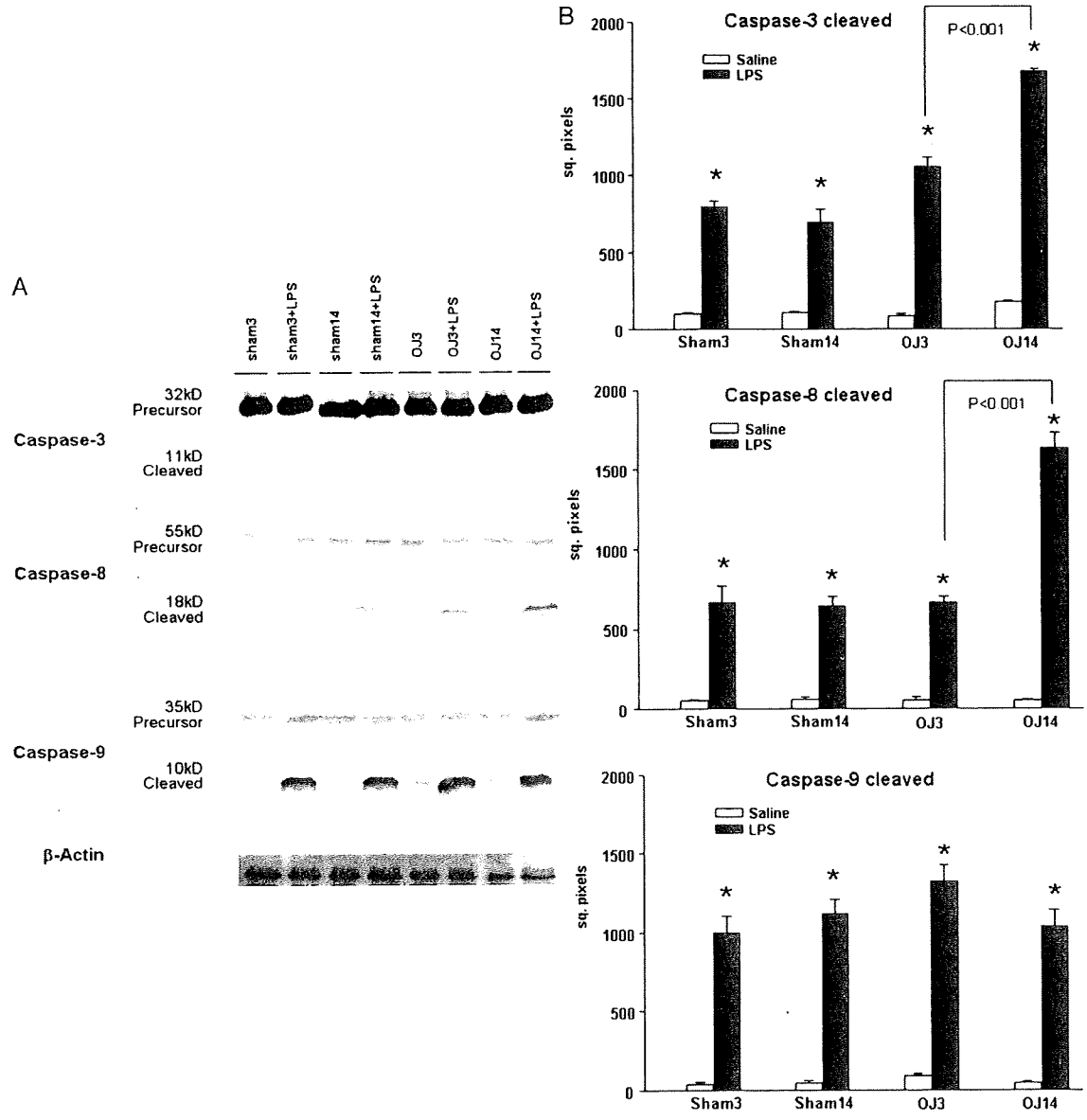

FIG. 3. **Effect of LPS administration on caspase 3, 8, and 9 expression.** A, Liver lysates obtained from the Sham3, Sham14, OJ3, and OJ14 at 3 h after LPS or saline administration was analyzed by Western blot. B, Results were quantitated by an image analysis of an autoradiogram. Data are mean ± SEM. *$P < 0.001$ vs. saline treatment. For all groups, n = 3.

multiple groups were analyzed with a one-way ANOVA, and individual group means were then compared with the Student-Newman-Keuls test. Overall survival was calculated by the Kaplan-Meier method, and comparisons were evaluated using the log-rank test. Differences were considered to be significant when $P < 0.05$.

RESULTS

Serum bilirubin levels and hepatic FasL expression

We assessed serum levels of T-BIL after bile duct ligation and division, and the T-BIL levels were elevated in mice at 3 days after bile duct ligation and division (OJ3) and significantly increased in mice at 14 days after bile duct ligation and division (OJ14) relative to that in mice at 3 days after the sham operation (Sham3) and at 14 days after the sham operation (Sham14), respectively (n = 5; Fig. 1A). Because apoptosis in OJ has been known to be involved in Fas stimulation (8), we analyzed the FasL expression in whole liver lysates during OJ by ELISA. The FasL expression significantly increased in OJ3 and OJ14 mice in comparison to the Sham3 and Sham14, respectively (n = 5; Fig. 1B).

Liver apoptosis, histological examination, and apoptotic pathway after LPS administration

Because PARP p85 fragment is an indicator for apoptosis, immunohistochemistry for PARP p85 fragment was performed to investigate whether hepatocyte apoptosis was induced. Poly (adenosine diphosphate–ribose) polymerase–positive apoptotic cells increased in OJ3 and OJ14 mice relative to the Sham3 and Sham14 (n = 6, respectively). At 3 h after LPS administration, significant hepatocyte apoptosis occurred in OJ14 mice relative to the OJ3 mice (Fig. 2, A, C, E, G, I, and K).

To assess whether hepatic injury increased after LPS administration, we examined histology by hematoxylin-eosin staining. Histological observations showed that a little focal necrosis was evident in OJ14 mice, whereas it more strongly increased in OJ14 mice at 3 h after LPS administration (Fig. 2, B, D, F, H, and J).

To determine the precise apoptosis pathway, we performed Western blot analysis to examine expression of precursor and cleaved caspases 3, 8, and 9. The expression of cleavage of caspases 3 and 8 at 3 h after LPS administration in OJ14 mice (n = 3, respectively) was increased more than those of the Sham3, Sham14, and OJ3 mice at 3 h after LPS administration (n = 3, respectively; Fig. 3, A and B). However, expression of cleavage of caspase 9 did not differ among the Sham3, Sham14, OJ3, and OJ14 after LPS administration (n = 3, respectively; Fig. 3, A and B).

Hepatic ATP content and serum ALT levels after LPS administration

Because apoptosis requires ATP, and a switch from apoptosis to necrapoptosis or secondary oncotic necrosis occurs when cells lack ATP (14), we assessed hepatic ATP content to determine whether apoptosis and necrapoptosis are induced in jaundiced mice after LPS administration. In OJ3 mice, ATP content significantly decreased and remained decreased in OJ14 relative to the Sham3 and Sham14, respectively (Fig. 4A; n = 6, respectively). At 3 h after LPS administration, ATP content significantly decreased in OJ14 mice in comparison to that in OJ3, Sham3, and Sham14, respectively (Fig. 4). Furthermore, ATP content in OJ14 mice with LPS treatment significantly decreased relative to OJ14 mice with saline treatment. On the contrary, ATP content after LPS administration in OJ3 mice was not statistically significantly different from mice with saline treatment (Fig. 4A). To determine whether hepatic injury was increased during OJ with LPS administration, we assessed serum levels of ALT. Serum ALT levels increased in OJ3 and OJ14 mice in comparison to the Sham3 and Sham14. At 3 h after LPS administration, serum ALT levels significantly increased in OJ14 mice in comparison to that in OJ3 (Fig. 4B).

Reduction in liver apoptosis after LPS administration in gld/gld mice

Because FasL has been known to activate death receptor leading to hepatocyte apoptosis and FasL increased during OJ in the current study, we used gld/gld mice that do not express FasL to investigate whether hepatocyte apoptosis occurred in OJ was induced by Fas. Number of PARP-positive apoptotic cells in gld/gld mice decreased in OJ3 and OJ14 mice relative to the wild-type mice (data not shown). In gld/gld mice, hepatocyte apoptosis significantly decreased after LPS administration in OJ14 mice relative to the wild-type mice (Fig. 5; n = 6, respectively).

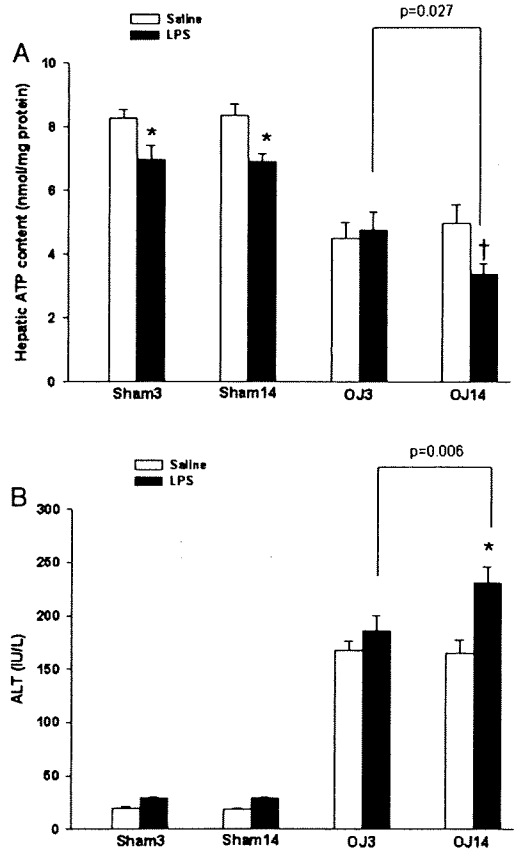

FIG. 4. **Effect of LPS administration on the liver ATP content and liver injury.** A, Hepatic ATP content was assessed by luminescence. Data are mean ± SEM. $^*P = 0.022$ vs. saline treatment. $^\dagger P = 0.034$ vs. saline treatment. For all groups, n = 6. B, Hepatocellular injury defined by serum levels of ALT. Data are mean ± SEM. $^*P < 0.001$ vs. saline treatment. For all groups, n = 6. Samples were obtained from the Sham3, Sham14, OJ3, and OJ14 mice at 3 h after LPS or saline administration.

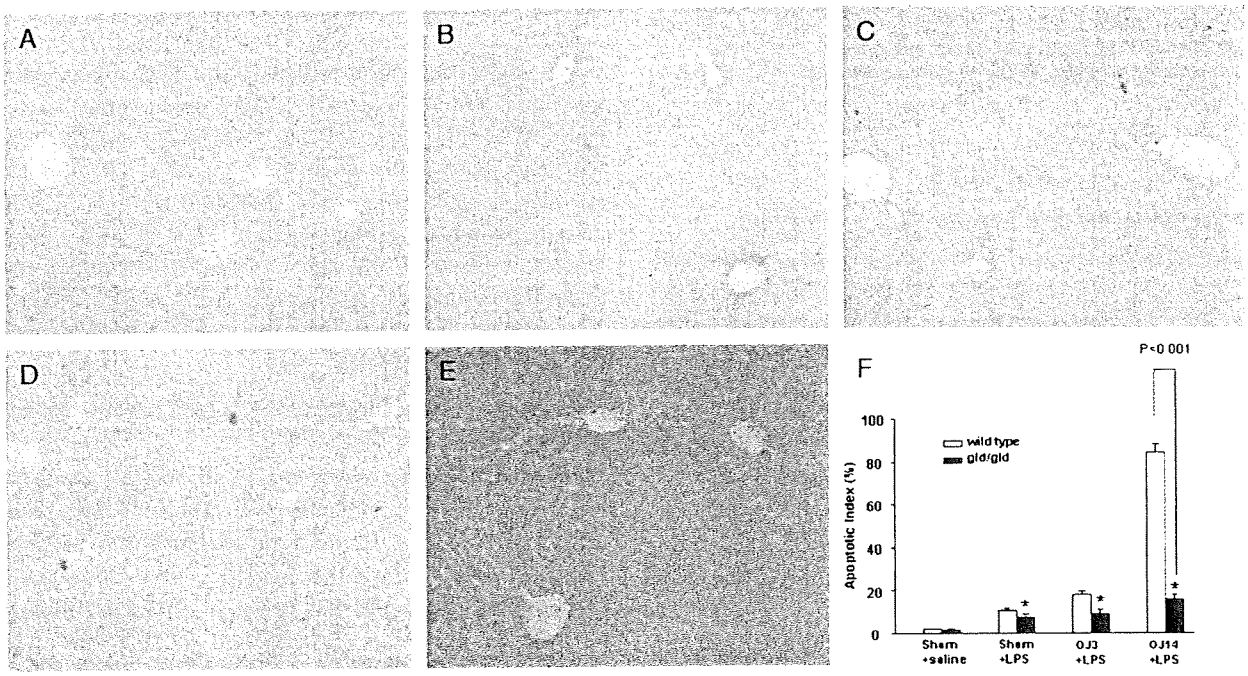

FIG. 5. **Hepatic apoptosis after LPS administration in gld/gld (FasL-deficient) mice.** Apoptosis was assessed by PARP p85 fragment immunohistochemistry (original magnification, 100×). Liver tissue obtained from the Sham14 (A) gld/gld mice at 3 h after saline administration. Liver tissue obtained from the Sham14 (B), OJ3 (C), and OJ14 (D) gld/gld mice at 3 h after LPS administration. Liver tissue obtained from OJ14 wild type (E) at 3 h after LPS administration. G, Apoptotic index of PARP p85. To calculate the apoptotic index, the number of stained and unstained hepatocytes was counted in five random fields (400×). Data are mean ± SEM. No significant difference was observed in the apoptotic index between the Sham3 and Sham14 gld/gld mice after LPS or saline administration. $^*P < 0.001$ vs. wild-type mice. For all groups, n = 6.

Survival after LPS administration in OJ

To determine the susceptibility to endotoxemia in OJ, wild-type and gld/gld mice were subjected to LPS administration (n = 5, respectively). The sham-operated mice receiving LPS were all alive longer than 24 h after LPS administration. OJ3 mice receiving LPS administration were all alive longer than 24 h after LPS administration, but all OJ14 mice receiving LPS administration died within 24 h after LPS administration. The survival rate in OJ14 gld/gld mice receiving LPS administration was significantly better than that in OJ14 wild-type mice receiving LPS administration (Fig. 6).

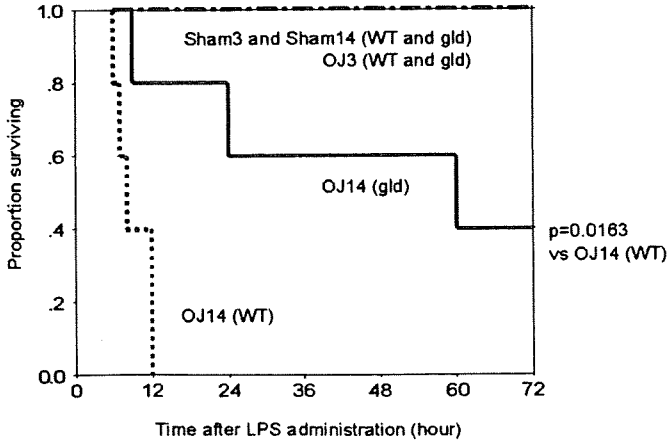

FIG. 6. **Survival after LPS administration in wild-type and gld/gld mice.** The Sham3, Sham14, OJ3, and OJ14 mice were treated with LPS administration (4 mg/kg, i.v.). For all groups, n = 5. Comparisons of overall survival were performed using the log-rank test.

DISCUSSION

Patients with OJ have bacteremic risk and may die of cholangitis or postoperative organ dysfunction after extended hepatectomy (15, 16). Acute cholangitis progresses from local infection to the systemic inflammatory response syndrome, leading to septic organ dysfunction. In contrast, Cherqui et al. (17) demonstrated that major liver resections without preoperative biliary drainage are safe in most patients with OJ. Although the morbidity rate in jaundiced patients was high in the study of Cherqui et al. (17), mortality rate was not so high. Their strategy was that surgery for jaundiced patients should be performed as soon as possible, suggesting that short periods of OJ might not affect remnant liver function after hepatectomy. Therefore, it is important to investigate whether hepatocyte injury differs over the time course of OJ with endotoxemia. Hepatocyte apoptosis has been defined as one of the causes of cholestatic liver injury (18, 19). An apoptotic body is engulfed by Kupffer cell, which stimulates ligand death, leading to cholestatic liver injury (20). The cholestatic liver is also known to be vulnerable to infection (21). Therefore, the current study showed that prolonged OJ sensitized the liver to LPS, thus leading to severe apoptosis and secondary necrosis (necrapoptosis).

Poly (adenosine diphosphate–ribose) polymerase p85 fragment, which results from caspase cleavage of PARP (116 kd), has been established as a hallmark of apoptosis (22, 23). The occurrence of hepatocyte apoptosis defined by immunohistochemistry for PARP p85 fragment after LPS administration was significantly enhanced in prolonged OJ. In an *in vitro* study, toxic bile salts cause hepatocyte apoptosis in a Fas- and

TRAIL-dependent manner (7, 24), and Fas has been reported to be involved in hepatocyte apoptosis in OJ (8, 25). The Fas-associated death domain promotes binding of procaspase 8 and its proteolytic activation to catalytic caspase 8. If sufficient amounts of caspase 8 are generated at the receptor, caspase 8 can directly activate procaspase 3 (9). Along with these findings, FasL expression increased during OJ, thus suggesting that Fas-FasL interaction is likely to play a role in hepatocyte apoptosis in OJ. The blockade of FasL using gld/gld mice reduced hepatocyte apoptosis, suggesting that FasL plays a crucial role in enhancing hepatocyte apoptosis in OJ with LPS administration.

The observation that caspase 9 activity is similarly increased in the Sham3, Sham14, OJ3, and OJ14 after LPS administration suggests that the mitochondrial permeability transition occurs by LPS administration. This is supported by the observation that in hepatocytes, the receptor signal needs to be amplified through mitochondria (18, 26). The balance between ATP depletion after the mitochondrial permeability transition and ATP generation determines the fate of cells as apoptotic or necrotic death (27). In the current study, hepatic ATP content significantly decreased, and PARP p85 fragment was strongly increased in OJ14 mice with LPS administration relative to the other mice. In acute cholestasis, Fas signaling and other alternations may lead to severe mitochondrial dysfunction and ATP depletion (28). This, along with the finding that the activation of PARP after cellular insults consumes a large amount of positive nicotinamide adenine dinucleotide, and in an effort to resynthesize positive nicotinamide adenine dinucleotide, may cause a massive ATP depletion (14). These findings suggest that prolonged OJ with LPS administration induces massive hepatic apoptosis and ATP depletion that in turn switches the cellular response to secondary oncosis (necrapoptosis), which is consistent with the findings that serum ALT levels were the highest and that focal necrosis was evident in the histopathological findings. OJ14 gld/gld mice after LPS administration prolonged survival in comparison to the wild-type mice, thus suggesting that the reduction in hepatocyte apoptosis caused by the blockade of FasL may contribute to attenuating subsequent necrapoptosis in prolonged OJ with LPS.

Concerns remain that enormous differences in hepatocyte apoptosis and the induction of caspase 8 after LPS administration were found between the short and prolonged periods of OJ (OJ3 and OJ14), although no significant difference was observed in the FasL expression between the OJ3 and OJ14 mice before LPS administration. These results suggested that other effects may also be at work to induce massive hepatocyte apoptosis in the prolonged periods of OJ. One possible candidate is TNF-α. TNF-α–associated death domains are known to promote the binding of procaspase 8 and subsequent proteolytic activation of catalytic caspase 8 (7, 25). The TNF-α expression in the OJ14 mice significantly increased after LPS administration relative to that observed in OJ3 mice, although there was no significant difference between the two groups before LPS administration (personal observation). It thus seems likely that TNF-α plays a certain role in the induction of hepatocyte apoptosis.

Fas ligand expression in normal tissues is restricted to T lymphocytes, macrophages, the cornea, the iris, ciliary bodies, the retina, and Sertoli cells (29, 30). The FasL expression in the current data seems to mirror our previous reports concerning hepatic accumulation of T lymphocytes and macrophages in OJ (31). Fas ligand is reported to play another role in induction of proinflammation (32). Furthermore, Canbay et al. (20) demonstrated that cholestatic liver injury tended to deteriorate after Kupffer cell engulfment of apoptotic bodies, which promotes inflammation and fibrogenesis. Thus, significant hepatocyte apoptosis is likely to induce inflammatory mediators. Our previous study showed that IL-1 significantly increased in OJ14 mice relative to OJ3 after LPS administration (31). This observation is consistent with the findings of Kennedy et al. (33), demonstrating an increased secretion of proinflammatory cytokines after LPS administration in the prolonged OJ. The increased expressions of proinflammatory mediators such as TNF-α and IL-1β may therefore enhance the systemic inflammatory responses, which may lead to a fatal outcome (34). Along with these findings, survival after LPS administration in the gld/gld mice intermediately ameliorated, but not completely, thus suggesting that prolonged periods of OJ may have other effects on survival in endotoxemia that are independent of FasL. Taken together, these data suggest that, in a clinical setting, longer biliary OJ may therefore increase organ dysfunction in endotoxemia that is caused by massive hepatocyte apoptosis and necrapoptosis. Up until recently, the mortality rates in severe cholangitis have still been reported to be more than 10%, and preoperative cholangitis is also known to be one of the risk factors of organ failure after hepatectomy (35). To reduce the risk, biliary drainage might therefore be an effective treatment modality in selected patients with OJ. However, the importance of preoperative biliary drainage has never been conclusively demonstrated in humans with OJ undergoing surgery. Furthermore, it is well known that an obstructive bile duct that has a biliary drainage tube put in place to relieve jaundice may increase the risk of infection. Therefore, some randomized clinical trials are presently underway to elucidate the necessity of biliary drainage in patients with OJ undergoing pancreatic head resection (36). From the current data, when patients undergo major hepatic resection, relief of biliary obstruction before surgery might therefore be required in patients who have prolonged cholestasis.

In conclusion, the current data suggested that the occurrence of hepatocyte apoptosis and secondary necrosis may differ during the time course of OJ with endotoxemia caused by FasL expression, caspase 8 activation, and significant ATP depletion. As a result, the liver in prolonged OJ may be fragile and therefore cause excessive apoptosis and necrapoptosis with endotoxemia.

REFERENCES

1. Pain JA, Cahill CJ, Bailey ME: Perioperative complications in obstructive jaundice: therapeutic considerations. *Br J Surg* 72:942–945, 1985.
2. Su CH, Tsay SH, Wu CC, Shyr YM, King KL, Lee CH, Lui WY, Liu TJ, P'eng FK: Factors influencing postoperative morbidity, mortality, and survival after resection for hilar cholangiocarcinoma. *Ann Surg* 223:384–394, 1996.
3. Dixon JM, Armstrong CP, Duffy SW, Davies GC: Factors affecting morbidity

and mortality after surgery for obstructive jaundice: a review of 373 patients. *Gut* 24:845–852, 1983.
4. Lipsett PA, Pitt HA: Acute cholangitis. *Surg Clin North Am* 70:1297–1231, 1990.
5. Nagino M, Kamiya J, Uesaka K, Sano T, Yamamoto H, Hayakawa N, Kanai M, Nimura Y: Complications of hepatectomy for hilar cholangiocarcinoma. *World J Surg* 25:1277–1283, 2001.
6. Belghiti J, Hiramatsu K, Benoist S, Massault P, Sauvanet A, Farges O: Seven hundred forty-seven hepatectomies in the 1990s: an update to evaluate the actual risk of liver resection. *J Am Coll Surg* 191:38–46, 2000.
7. Faubion WA, Guicciardi ME, Miyoshi H, Bronk SF, Roberts PJ, Svingen PA, Kaufmann SH, Gores GJ: Toxic bile salts induce hepatocyte apoptosis via direct activation of Fas. *J Clin Invest* 103:137–145, 1999.
8. Miyoshi H, Rust C, Roberts PJ, Burgart LJ, Gores GJ: Hepatocyte apoptosis after bile duct ligation in the mouse involves Fas. *Gastroenterology* 117:669–677, 1999.
9. Peter ME, Krammer PH: Mechanisms of CD95(APO-1/Fas)-mediated apoptosis. *Curr Opin Immunol* 10:545–551, 1998.
10. Yerushalmi B, Dahl R, Devereaux MW, Gumpricht E, Sokol RJ: Bile acid–induced rat hepatocyte apoptosis is inhibited by antioxidants and blockers of the mitochondrial permeability transition. *Hepatology* 33:616–626, 2001.
11. Wang X: The expanding role of mitochondria in apoptosis. *Genes Dev* 15:2922–2933, 2001.
12. Jaeschke H, Lemasters JJ: Apoptosis versus oncotic necrosis in hepatic ischemia/reperfusion injury. *Gastroenterology* 125:1246–1257, 2003.
13. Takeuchi D, Yoshidome H, Kato A, Ito H, Kimura F, Shimizu H, Ohtsuka M, Morita Y, Miyazaki M: Interleukin 18 causes hepatic ischemia/reperfusion injury by suppressing anti-inflammatory cytokine expression in mice. *Hepatology* 39:699–710, 2004.
14. Schwabe RF, Brenner DA: Mechanisms of liver injury. I. TNF-alpha–induced liver injury: role of IKK, JNK, and ROS pathways. *Am J Physiol Gastrointest Liver Physiol* 290:G583–G589, 2006.
15. Nimura Y, Kamiya J, Kondo S, Nagino M, Uesaka K, Oda K, Sano T, Yamamoto H, Hayama N: Aggressive perioperative management and extended surgery for hilar cholangiocarcinoma: Nagoya experience. *J Hepatobiliary Pancreat Surg* 7:155–162, 2000.
16. Kawasaki S, Imamura H, Kobayashi A, Noike T, Miwa S, Miyagawa S: Results of surgical resection for patients with hilar bile duct cancer: application of extended hepatectomy after biliary drainage and hemihepatic portal vein embolization. *Ann Surg* 238:84–92, 2003.
17. Cherqui D, Benoist S, Malassagne B, Humeres R, Rodriguez V, Fagniez PL: Major liver resection for carcinoma in jaundiced patients without preoperative biliary drainage. *Arch Surg* 135:302–308, 2000.
18. Rodrigues CM, Steer CJ: Mitochondrial membrane perturbations in cholestasis. *J Hepatol* 32:135–141, 2000.
19. Patel T, Gores GJ: Apoptosis and hepatobiliary disease. *Hepatology* 21: 1725–1741, 1995.
20. Canbay A, Feldstein AE, Higuchi H, Werneburg N, Grambihler A, Bronk SF, Gores GJ: Kupffer cell engulfment of apoptotic bodies stimulates death ligand and cytokine expression. *Hepatology* 38:1188–1198, 2003.
21. Greve JW, Gouma DJ, Soeters PB, Buurman WA: Suppression of cellular immunity in obstructive jaundice is caused by endotoxins: a study with germ-free rats. *Gastroenterology* 98:478–485, 1990.
22. Duriez PJ, Shah GM: Cleavage of poly (ADP-ribose) polymerase: a sensitive parameter to study cell death. *Biochem Cell Biol* 75:337–349, 1997.
23. Simbulan-Rosenthal CM, Rosenthal DS, Iyer S, Boulares AH, Smulson ME: Transient poly(ADP-ribosyl)ation of nuclear proteins and role of poly(ADP-ribose) polymerase in the early stages of apoptosis. *J Biol Chem* 273: 13703–13712, 1998.
24. Schmucker DL, Ohta M, Kanai S, Sato Y, Kitani K: Hepatic injury induced by bile salts: correlation between biochemical and morphological events. *Hepatology* 12:1216–1221, 1990.
25. Power C, Fanning N, Redmond HP: Cellular apoptosis and organ injury in sepsis: a review. *Shock* 18:197–211, 2002.
26. Yin XM: Bid, a critical mediator for apoptosis induced by the activation of fas/TNF-R1 death receptors in hepatocytes. *J Mol Med* 78:203–211, 2000.
27. Leist M, Single B, Castoldi AF, Kühnle S, Nicotera P: Intracellular adenosine triphosphate (ATP) concentration: a switch in the decision between apoptosis and necrosis. *J Exp Med* 185:1481–1486, 1997.
28. Malhi H, Gores GJ, Lemasters JJ: Apoptosis and necrosis in the liver: a tale of two deaths? *Hepatology* 43:S31–S44, 2006.
29. Griffith TS, Brunner T, Fletcher SM, Green DR, Ferguson TA: Fas ligand-induced apoptosis as a mechanism of immune privilege. *Science* 270: 1189–1192, 1995.
30. Chen JJ, Sun Y, Nabel GJ: Regulation of the proinflammatory effects of fas ligand (CD95L). *Science* 282:1714–1717, 1998.
31. Morita Y, Yoshidome H, Kimura F, Shimizu H, Ohtsuka M, Takeuchi D, Mitsuhashi N, Iida A, Miyazaki M: Excessive inflammation but decreased immunological response renders liver susceptible to infection in bile duct ligated mice. *J Surg Res* 146:262–270, 2008.
32. Faouzi S, Burckhardt BE, Hanson JC, Campe CB, Schrum LW, Rippe RA, Maher JJ: Anti-Fas induces hepatic chemokines and promotes inflammation by an NF-kappa B–independent, caspase-3–dependent pathway. *J Biol Chem* 276:49077–49082, 2001.
33. Kennedy JA, Clements WD, Kirk SJ, McCaigue MD, Campbell GR, Erwin PJ, Halliday MI, Rowlands BJ: Characterization of the Kupffer cell response to exogenous endotoxin in a rodent model of obstructive jaundice. *Br J Surg* 86: 628–633, 1999.
34. Minutoli L, Altavilla D, Bitto A, Polito F, Bellocco E, Laganà G, Giuliani D, Fiumara T, Magazù S, Ruggeri P, et al.: The disaccharide trehalose inhibits proinflammatory phenotype activation in macrophages and prevents mortality in experimental septic shock. *Shock* 27:91–96, 2007.
35. Nagino M, Nimura Y, Hayakawa N, Kamiya J, Kondo S, Sasaki R, Hamajima N: Logistic regression and discriminant analysis of hepatic failure after liver resection for carcinoma of the biliary tract. *World J Surg* 17:250–255, 1993.
36. van der Gaag NA, de Castro SM, Rauws EA, Bruno MJ, van Eijck CH, Kuipers EJ, Gerritsen JJ, Rutten JP, Greve JW, Hesselink EJ, et al.: Preoperative biliary drainage for periampullary tumors causing obstructive-jaundice; DRainage vs. (direct) OPeration (DROP-trial). *BMC Surg* 7:3, 2007.

Journal of Surgical Research 152, 118–127 (2009)
doi:10.1016/j.jss.2008.01.027

Preoperative GATA3 mRNA Expression in Peripheral Blood Mononuclear Cells is Up-Regulated in Patients With Postoperative Infection Following Hepatobiliary Pancreatic Surgery

Jun Kawamoto, M.D., Fumio Kimura, M.D.,[1] Hideyuki Yoshitomi, M.D., Hiroaki Shimizu, M.D., Hiroyuki Yoshidome, M.D., Masayuki Ohtsuka, M.D., Atsushi Kato, M.D., Satoshi Nozawa, M.D., Katsunori Furukawa, M.D., Noboru Mitsuhashi, M.D., Dan Takeuchi, M.D., and Masaru Miyazaki, M.D.

Department of General Surgery, Chiba University Graduate School of Medicine, Chiba, Japan

Submitted for publication November 7, 2007

Background. **Aggressive hepatobiliary pancreatic surgery has been associated with high complication rates. Correlations of Th1/Th2 balance and toll-like receptor (TLR) 2/4 expression with postoperative infection following surgery were prospectively evaluated.**

Methods. **Plasma concentrations of interleukin (IL)-6, IL-10, soluble lymphocyte activation gene (sLAG)-3, and soluble CD30 were determined by enzyme-linked immunosorbent assay, and expression levels of T-bet, GATA-3, TLR2, and TLR4 mRNA in peripheral blood mononuclear cells were assayed by reverse transcription-polymerase chain reaction perioperatively in 56 consecutive patients who underwent hepatobiliary pancreatic surgery.**

Results. **Of the 56 patients, 30 patients had postoperative infection. Postoperative plasma levels of IL-6 and IL-10 were significantly higher in patients with postoperative infection than in those without infection ($P < 0.05$). Plasma soluble CD30 level and GATA-3 mRNA expression level were significantly higher preoperatively, and remained higher by postoperative d 7 in patients with postoperative infection ($P < 0.05$). Soluble lymphocyte activation gene levels were not significantly different between the two groups. T-bet mRNA expression level was significantly higher on postoperative d 3, 7, and 14 in patients with postoperative infection ($P < 0.05$). Preoperative expression levels of GATA-3 mRNA correlated significantly with those of TLR2 and TLR4 mRNA ($P < 0.05$).**

Conclusions. **These results suggest that in patients with postoperative infection, Th1/Th2 balance shifts toward Th2 dominance preoperatively.**

Key Words: **hepatobiliary pancreatic surgery; postoperative infection; Th1/Th2 balance; T-bet; GATA3; TLRs; soluble CD30.**

INTRODUCTION

An aggressive surgical approach to achieve R0 resection has resulted in improved survival for patients with advanced hepatobiliary pancreatic malignancies [1, 2]. However, aggressive hepatobiliary pancreatic surgery, especially extended liver resection and radical pancreaticoduodectomy have been associated with high complication rates of 40% to 50% [1, 3–5]. Most common complications following major hepatobiliary pancreatic surgery are septic complications, including cholangitis, wound infection, pneumonia, intra-abdominal abscess, fistula, and septicemia [1, 3–5].

It has been reported that sever trauma and hemorrhage cause prolonged immunosuppression and increase the susceptibility to sepsis [6, 7]. In humans, major trauma causes a marked decrease in interleukin (IL)-12 and interferon-gamma production and an increase in IL-4 and IL-10 production by peripheral blood mononuclear cells (PBMCs), and shifts the type 1/2 helper T cell (Th1/Th2) balance toward Th2 dominance, promoting the susceptibility to infection [8–10]. Furthermore, it has been reported that sever inflammation induces alternatively activated macrophages with no antibacterial capabilities, whereas mild inflammation induces classically activated macrophages, effector cells for the antibacterial innate immunity

[1] To whom correspondence and reprint requests should be addressed at Department of General Surgery, Chiba University Graduate School of Medicine, 1-8-1 Inohana, Chuo-ku, Chiba 260-8670, Japan. E-mail: kimura-f@umin.net.

0022-4804/09 $36.00

against pathogens [11]. In patients undergoing an aggressive surgery, therefore, sever tissue injury due to complicated surgical procedures and perioperative blood transfusion may also modulate the innate and adapted immune response of the host, and induce systemic anergy resulting in postoperative septic complications [12].

Toll-like receptors (TLRs) play a pivotal role not only in innate immune response but also in regulation of Th1/Th2 balance [13]. It is well known that recognition of specific pathogen associated molecular patterns is mediated primarily by TLRs [13]. Also, the type of TLR stimulation during the initial phase of immune activation determines the polarization of the adaptive immune response [13]. It has been reported that TLR2 expression on CD14+ peripheral blood monocytes is significantly up-regulated in patients with cirrhosis [14]. Furthermore, tissue expression of TLR-4 in the small intestine and liver is up-regulated in patients with obstructive jaundice [15]. These reports suggest that, in patients undergoing hepatobiliary pancreatic surgery, underlying hepatobiliary diseases potentially modulate TLRs expression and Th1/Th2 balance in the perioperative period.

The purpose of this study is to assess the effects of hepatobiliary pancreatic surgery on expression level of the principal transcription factors for the differentiation of Th1/Th2 (T-bet and GATA-3 mRNA) and TLR2/4 mRNA in PBMCs, and to clarify the association of these immunological parameters with postoperative infectious complications following surgery.

PATIENTS AND METHODS

From September 2005 through May 2006, 56 consecutive patients undergoing surgery for hepatobiliary pancreatic malignancy were studied (24 women, 32 men; age range 38 to 81 y, median 63.5). The subjects included 19 patients with primary liver cancer (hepatocellular carcinoma in 14, intrahepatic cholangiocellular carcinoma in 5), 4 patients with hepatic metastases (from colorectal cancer in 3, gastric cancer in 1), 16 patients with biliary tract cancers (bile duct cancer in 12, gallbladder cancer in 4), 14 patients with pancreatic invasive ductal carcinoma, 2 patients with intraductal papillary mucinous neoplasm, and 1 patients with duodenal cancer. Of the 56 patients studied, 28 had normal hepatic parenchyma, 8 had cirrhotic liver, and 20 had jaundiced liver. All of the jaundiced patients underwent biliary drainage before surgery (percutaneous transhepatic biliary drainage in 14, endoscopic naso-biliary drainage in 4, endoscopic retrograde biliary drainage in 2). Drainage interval ranged from 11 to 65 d with median interval of 44 d. Of the 20 patients, 18 had positive bile culture before surgery. Hepatobiliary pancreatic surgeries performed in these patients included 4 extended right hepatectomies, 2 right hepatectomies, 5 extended left hepatectomies, 2 left hepatectomies, 11 sectionectomies, 9 segmentectomies, 19 pancreaticoduodenectomies, and 4 distal pancreatectomies. All of the patients had intraperitoneal closed drainage placed and received prophylactic antibiotics just before and after operation, and twice a day on postoperative d 1 and 2. Thirty-eight patients received cefmetazole sodium 2000 mg/d while 18 patients with positive bile culture received effective antibiotics according to the sensitivity of isolated bacterial species. Patients with postoperative infection received additional antibiotic treatment according to the sensitivity of the bacterial species isolated from infection site. No patient was on total parenteral nutrition before surgery. All patients were on total parenteral nutrition for at least 3 d after surgery before starting oral intake.

Peripheral venous blood samples were collected from all patients before surgery (baseline measurements), immediately after surgery (d 0), and on postoperative d 1, 3, 7, and 14. Whole blood samples were collected into the cell preparation tube (BD Vacutainer CPT; Becton Dickinson, Franklin Lakes, NJ), and plasma and PBMCs were isolated. Plasma concentrations of interleukin IL-6, IL-10, soluble lymphocyte activation gene (sLAG) -3, and soluble CD30 (sCD30) were determined by enzyme-linked immunosorbent assay (ELISA), and expression levels of T-bet, GATA-3, TLR2, and TLR4 mRNA in PBMCs were assayed by the quantitative reverse transcription-polymerase chain reaction (RT-PCR).

Interactions of these immunological parameters and perioperative clinical parameters with postoperative infectious complications were analyzed. Perioperative clinical parameters included age, gender, hepatic histology, indocyanine green retention at 15 min (ICG R15), serum albumin level, total cholesterol level, cancer stage, operative procedures, operating time, blood loss, and length of postoperative hospital stay. This protocol was approved by the Ethics Committee of our institute. Informed consent was obtained from all patients studied.

Definition of Postoperative Infectious Complications

The definitions of infectious complications were as follows: pneumonia, lobar pneumonia with culture positive sputum; intra-abdominal abscess, radiologically proven abscess cavity with culture positive fluid; wound infection, the wound is broken down, gaping or completely dehisced; and cholangitis, fever (>38°C) and culture positive bile. Infectious complications were bacteriologically confirmed in all patients. Dysfunctions of the respiratory, renal, hepatic, cardiovascular, hematologic, and neurological systems were defined as the PO2:FiO2 ratio less than 150, serum creatinine level more than 350 μmol/L, serum bilirubin level more than 240 μmol/L, hypotension or the need for inotropic support, platelet count less than 5 × 104/μL, and coma or obtundation, respectively.

PBMCs Sampling

The cell preparation tube combines a blood collection tube containing sodium citrate as an anticoagulant with a Ficoll-Hypaque density fluid and a polyester gel barrier, which separates the two liquids (BD Vacutainer; Becton Dickinson). Whole blood samples collected into the cell preparation tube were subjected to density gradient centrifugation. Isolated plasma samples were stored at −80°C until tested. The isolated PBMCs were washed twice with phosphate-buffered saline and the cells counted. The PBMCs were resuspended at 5×10^6/mL in freezing media (90% heat inactivated fetal calf serum, 10% dimethyl sulfoxide) and stored at −80°C until tested.

Measurement of Plasma Cytokine Levels

Plasma levels of IL-6 and IL-10 were determined using ELISA kit purchased from R and D Systems (Minneapolis, MN). sLAG-3 was determined using ELISA development kit purchased from Apotech Corporation (Epalinges, Switzerland). sCD30 was determined using ELISA kit purchased from Bender Med Systems (Vienna, Austria).

RNA Isolation, cDNA Synthesis, and Quantitative RT-PCR

Total RNA from PBMCs was extracted by the Qiagen spin column method (RNeasy mini kit; Qiagen, Tokyo, Japan) exactly as described in the manufacturer's protocol manual. cDNA was synthesized from total RNA using the T-Primed First-Strand Kit for RT-

PCR (Amersham Biosciences United Kingdom, Little Chalfont, United Kingdom). Expression of T-bet, GATA3, TLR2, TLR4, and glyceraldehyde-3-phosphate dehydrogenase (GAPDH) mRNA, a house-keeping gene, was detected by the quantitative RT-PCR method using Light-Cycler with Light Cycler-Fast Start DNA Master SYBR Green I kit (Roche Diagnostics, Mannheim, Germany). RT-PCR was performed with the following primer sets; T-bet: forward 5′-GTCAATTCCTTGGGGGAGAT-3′, reverse 5′-TCATGCTGACTGCTCGAAAC-3′, GATA3: forward 5′-CTGGCCACAGTTGTTTCATG-3′, reverse 5′-GCAACTGGTGAACGGTAACA-3′ TLR2: forward 5′-AGAACAATGATGCTGCCA-3′, reverse 5′-CAGCTCTCAGATTTACCCAA-3′, TLR4: forward 5′-CCTGGACCTGAGCTTTAATC-3′, reverse 5′-CTGATATGCCCCATCTTCAA-3′, and GAPDH: forward 5′-ACCCAGAAGACTGTGGATGG-3′, reverse 5′-TTCTAGACGGCAGGTCAGGT-3′. The conditions for quantitative RT-PCR were as follows: PCR was performed with an initial denaturation step at 95°C for 10 min, followed by 45 cycles denaturation at 95°C for 10 s, annealing for 10 s (at 55°C for TLR2, 58°C for TLR4 and T-bet, 60°C for GATA3), extension at 72°C for 7 s, and GAPDH under the aforementioned conditions, except with extension at 72°C for 8 s. TLR2, TLR4, T-bet, GATA3, and GAPDH mRNA levels were determined as the absolute number of copies normalized against GAPDH mRNA copy number.

Statistical Analysis

Results are expressed as mean ± SD. Paired and unpaired Student's *t*-tests were used to analyze paired and unpaired samples, respectively. The χ^2 method was used to assess significance between proportions. Simple linear regression analysis was performed to assess the correlations between the immunological and clinical parameters. Binary logistic regression analysis was used to define associations between the immunological and clinical parameters and clinical outcome. For this analysis, countable variables were divided into two groups by using the median value as a cutoff point. A *P*-value < 0.05 was considered statistically significant.

RESULTS

Postoperative Infectious Complications

Thirty of the 56 subjects developed postoperative infectious complications, including wound infection in 18, intra-abdominal abscess in 18, cholangitis in 6, pneumonia in 5. All of the 30 patients with postoperative infection had surgical site infection (SSI). SSI was superficial incisional in 3, deep incisional in 1, and organ/space infection in 26. Of the 30 patients with postoperative infection, 4 had organ dysfunction. One patient had a single failing organ (hepatic system) and survived. The remaining 3 patients had multiple organ dysfunctions. The failing organs were respiratory system in 3, hepatic system in 3, renal system in 3, cardiovascular system in 2, hematologic system in 2. Of the 3 patients, 2 died within 30 d after surgery. Overall morbidity and mortality rates for all patients in the study were 54% and 4%, respectively.

Perioperative and Operative Parameters

Patients with postoperative infection had significantly lower serum albumin level ($P = 0.0359$), longer operation time ($P = 0.0060$), larger volume of blood loss at the operation ($P = 0.0056$), and longer length of postoperative hospital stay ($P = 0.00001$) than those without postoperative infection. There were no significant differences between the two groups as to age, gender ratio, hepatic histology, ICG R15, total cholesterol, cancer stage, and operative procedures (Table 1). In 8 of the 18 patients with preoperative positive bile culture, bacteria isolated from bile was responsible for

TABLE 1

General Characteristics of the Patients

Parameters	Patients with postoperative infection ($n = 30$)	Patients without postoperative infection ($n = 26$)	*P* value
Age (y)	64.0 ± 9.1	64.1 ± 11.4	N.S.
Gender (male/female)	19/16	13/8	N.S.
Hepatic histology (Normal: cirrhosis: jaundice)	10: 5: 15	18: 3: 5	N.S.
Preoperative biliary drainage (yes/no)	14/16	6/20	N.S.
ICG R15* (%)	13.7 ± 7.3	17.7 ± 11.7	N.S.
Albumin* (g/dL)	3.7 ± 0.5	4.0 ± 0.5	0.0359
Total cholesterol* (mg/dL)	166.6 ± 50.3	188.8 ± 52.1	N.S.
Cancer stage (UICC) (Stages I, II: Stages III, IV)	4: 26	6: 20	N.S.
Operative procedure (Liver: Pancreas)	14: 16	16: 10	N.S.
Operation time (min)	472 ± 135	326 ± 108	0.0060
Blood transfusion (yes/no)	11/19	6/20	N.S.
Blood loss (g)	1665 ± 1753	735 ± 518	0.0056
Hospital stay (d)	50.6 ± 24.0	23.7 ± 11.6	0.0001

Notes. Results are presented as mean ± SD or ratio. Student's *t*-test was used to analyze unpaired samples. The χ^2 method was used to assess significance between proportions.

Normal = normal liver parenchyma; cirrhosis = cirrhotic liver; jaundice = jaundiced liver; ICG-R15 = indocyanine green retention at 15 min; UICC = International Union Against Cancer; Liver = liver resection; pancreas = pancreatoduodenectomy or distal pancreatectomy.

* Preoperative values.